ISSN 1882-3432

TECHNOLOGY DEVELOPMENT CENTER NEWS

NATIONAL INSTITUTE OF INFORMATION AND COMMUNICATIONS TECHNOLOGY

Serial No. 39 January 2021

CONTENTS

Proceedings of the 18th NICT TDC Symposium (Kashima, October 1, 2020)

KNIFE, Kashima Nobeyama InterFErometer

Makoto Miyoshi (*makoto.miyoshi@nao.ac.jp*)

National Astronomical Observatory, Japan, 2-21-1, Osawa, Mitaka, Tokyo, Japan, 181-8588

Abstract: By connecting two antennas, Kashima 34 m and Nobeyama 45 m, an east-west baseline of 200 km is formed. At that time, because Nobeyama 45 m had the world's number one sensitivity in the 43 GHz band, and also Kashima 34 m was the world's third-largest one, the Kashima-Nobeyama baseline provided the highest sensitivity at 43 GHz VLBI (Figure 1). The construction of the Kashima 34 m antenna began in 1988, also almost at the same time, a domestic project of mm-VLBI (KNIFE, Kashima Nobeyama INterFrermeter) started. Nobeyama Radio Observatory provided the first cooled-HEMT 43 GHz receiver in the world to the Kashima 34 m. In October 1989, the first fringe at 43 GHz was detected. We here review the achievements of the KNIFE at that time.

1. KNIFE project

In 1987, the Radio Research Laboratory (RRL, NICT at present) decided to construct the Kashima 34 m antenna as the main station of the Western Pacific interferometer. At that time, the Nobeyama Radio Observatory, a branch of the National Astronomical Observatory of Japan (NAOJ) participated in the global millimeter-wave VLBI using the Nobeyama 45 m and had just started VLBI observations. A set of Mark-3 recorder was brought to the Usuda station from Nobeyama, and the first space VLBI experiment with the TDRS satellite was conducted using Usuda 64 m, and the fringe detection was successful. However, in Japan, independent astronomical VLBI observational research has not yet been possible. In response to the news of the construction of the Kashima 34 m antenna, Prof. Morimoto (Figure 2) noticed that the Kashima 34 m antenna has a surface accuracy of 170 μas and that it is very effective for millimeter-wave VLBI observation. Prof. Morimoto proposed to RRL to conduct the millimeter-wave VLBI researches in collaboration with NAOJ, and the joint research began. Using the 43 GHz cooling receiver dewar owned by RRL, NAOJ decided to manufacture the world's first 43 GHz cooled HEMT receiver (Figure 3) and the joint research started in 1989. The KNIFE experiment started at the same time as the start-up and test of the 34 m antenna. Though the first KNIFE experiment on June 14-15, 1989 failed, at the second KNIFE experiment on October 20-22, 1989, the first 43 GHz fringes were successfully detected from the observations of the strong SiO masers in Orion KL and VY CMa.

2. SiO maser observations

The SiO maser emissions originate at circumstellar envelopes of late-type stars, but they were mysterious phenomena at that time. VLBI observations of SiO masers had been carried out, but the angular size of SiO maser was quite large, and then resolve-outs were occurred at long baselines, so the structures of SiO masers were not well understood. The KNIFE baseline is 200 km. At 43 GHz, the minimum fringe spacing is about 7 mas, so it is just suitable for observing SiO masers. Prof. Morimoto urged the install of the 43 GHz receiver on the Kashima 34 m antenna as soon as possible because fruitful scientific results were expected.

The Figure 4 shows the observational result of SiO maser by KNIFE. The star itself cannot be detected, but the SiO masers are distributed around the star. The distributions of SiO masers with $v = 1$ and $v = 2$, though their excitation temperatures differ about 1800 K, are almost the same as each other. This means that the maser is inferred to be due to collisional excitation [1]. At that time, the VLBA in USA was in the process of being constructed, but SiO maser observations were performed as a test. Panel (e) in the Figure 4 shows the VLBA result (SiO masers in U Her [2]). If compared to the result of SiO masers by the VLBA four stations, It can be understood that the KNIFE performance was considerably good even though it was a single baseline.

3. Observations of high velocity water mega maser in NGC 4258

In 1992, Nakai et al. discovered high-velocity components in the water mega maser of the galaxy NGC 4258 by using the Nobeyama 45 m in Japan [3]. Relative to the known water maser components, they show velocity shifts of ±1000 km/s. There are two groups, one shows blue shifts of about 1000 km/s while the other shows red shifts of about 1000 km/s. Hearing the news, Prof. Morimoto said, "If the masers move with velocities about 1000 km/s, we can easily detect the proper motions of the maser components. Observe with Kashima 34 m immediately! Observe twice so as not to fail!" What is the origin of the high-velocity mega masers of NGC 4258? In order to identify the origin, observations with a high spatial resolution are required. Prof. Morimoto suggested that we should investigate with KNIFE as soon as

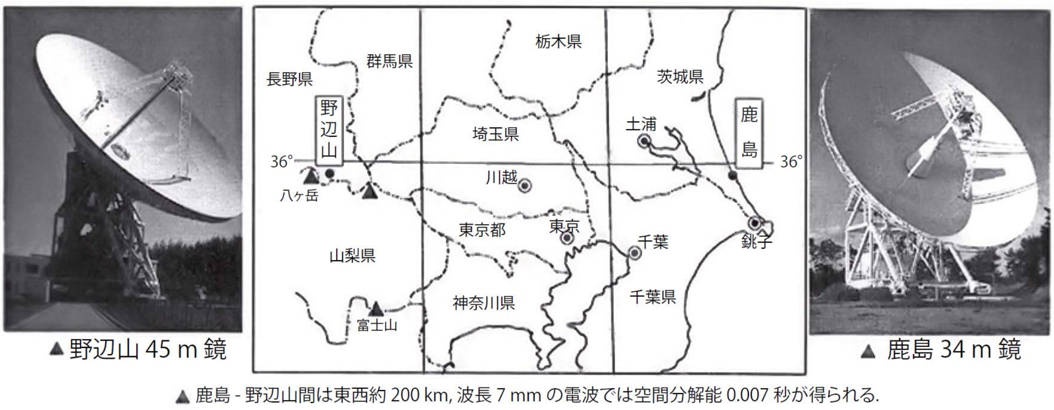

Figure 1. KNIFE baseline: The baseline length is 197.66 km. The north-south component is only 240 m. The fringe spacing is about 7 mas at 43 GHz observations, suitable for SiO maser observations.

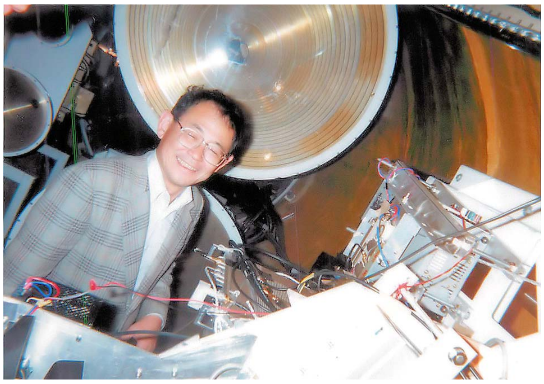

Figure 2. Prof. Masaki Morimoto, who promoted the KNIFE project.

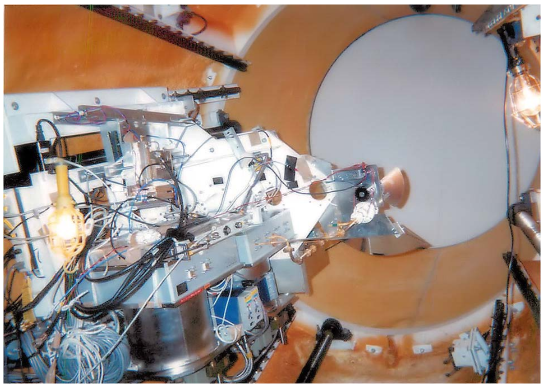

Figure 3. The cooled HEMT Receiver installed to 34 m telescope. This photo was taken at the time when the first 43 GHz fringe was detected in Oct. 1989.

possible. The KNIFE observations were conducted in early June 1993, less than a month after the discovery. However, due to calculation errors of the observational sky frequencies, correlations by new NAOCO correlator in NAOJ [4] that has not even been bug-fixed, and the use of imaging software made tentatively, it was not possible to find the maser distributions exactly. However, in August 1993, it is found that the high-velocity components are also located at the center of the galaxy, within 50 mas of the known main components. In 1995, VLBA observations revealed that the water mega maser in NGC 4258 was from a molecular gas disk with Keplerian motion around a supermassive black hole. From the maser velocity and structure, the mass of the black hole is estimated to be $3.6 \times 10^7 M_\odot$ [5]. The Figure 5 shows the mega maser distribution obtained from reanalyzing the KNIFE data and that from the result of VLBA. As you can see from the Figure, it is possible to capture the structure of the water mega maser in NGC 4258 even with the single 200 km baseline of KNIFE. The KNIFE observation of NGC 4258 also shows the excellent performance of the KNIFE.

4. The role played by the KNIFE project

The results are not only those mentioned above. Pioneering research was conducted on higher-frequency geodetic VLBI using KNIFE [7]. In addition, survey observations of water and SiO masers were carried out using the single Kashima 34 m antenna and KNIFE [8], [9]. The KNIFE astronomical observations using the single-baseline between Kashima 34 m and Nobeyama 45 m were carried out until 1992. In 1993 it developed into J-Net observations with 4 stations including Mizusawa 10 m antenna and Kagoshima 6 m antenna; Monitoring VLBI observations of the burst phenomena of water masers in Orion KL were performed before its beginning by chance [10]. KNIFE paved the way for the subsequent development of astronomical VLBI researches in Japan.

References

[1] Miyoshi, M., Matumoto, K., Kameno, S., Takaba, H., & Iwata, T., Collisional Pumping of SiO Masers in Evolved Stars, *Nature*, **371**, 395-397, 1994.

[2] Diamond, P. J., Kemball, A. J., Junor, W., Zensus, A., Benson, J., & Dhawan, V., Observation of a Ring Structure in SiO Maser Emission from Late-Type Stars, Astrophysical Journal Letters v.430, p.L61, 1994.

[3] Nakai, N., Inoue, M., & Miyoshi, M., Extremely-high-velocity H_2O maser emission in the galaxy NGC 4258, *Nature*, **361**, 45-47, 1993.

[4] Shibata, K., Sasao, T., Kawaguchi, N., Tamura, Y., Kameno, S., Miyoshi, M., Asari, K., Manabe, S., Hara, T., Kuji, S., Sato, K., Miyaji, M., Matumoto, K., Asaki, Y., Yasuda, S., & Nakamura, S., A New Advanced One-Unit VLBI Correlator (NAOCO), Proceedings of the International Symposium Held at Kyoto International Conference Hall on September 6-10, 1993 'VLBI TECHNOLOGY Progress and Future Observational Possibilities' 327-331, Sasao, T., Manabe, S., Kameya, O. & Inoue, M. eds. Terra Scientific Publishing Company, 1994.

[5] Miyoshi, M., Moran, J., Herrnstein, J., Greenhill, L., Nakai, N., Diamond, P., & Inoue, M., Evidence for a Black Hole from High Rotation Velocities in a Sub-Parsec Region of NGC 4258, *Nature*, **373**, 127-129, 1995.

[6] Herrnstein, J.R., Moran, J., Greenhill, L., Diamond, P., Inoue, M., Nakai, N., Miyoshi, M., Henkel, C.,& Riess,A., A geometric distance to the galaxy NGC 4258 from orbital motions in a nuclear gas disk, *Nature*, **400**, 539-541, 1999.

[7] Matumoto, K., Kawaguchi, N., Inoue, M., Miyoshi, M., Kameno, S., Takaba, H., Iwata, T., & Kurihara, N., A Radio Source Survey at 22 and 43 GHz for Geodetic VLBI, *Journal of the Geodetic Society of Japan*, **40**, 255-265, 1994

[8] Takaba, H., Ukita, N., Miyaji, T., & Miyoshi, M., Spectral Evolution of H_2O Maser in Late Type Stars, *Publ. Astron. Soc. Japan*, **46**, 1-14, 1994.

[9] Imai, H., Miyoshi, M., Ukita, N., Morimoto, M., Iwata, T., Takaba, H., Kameno, S., Matumoto, K., Fujisawa, K., & Kawaguchi, N., Snapshot VLBI Observations of SiO $v = 1$ and $v = 2$ (J=1-0) Maser Sources. *Publ. Astron. Soc. Japan*, **53**, 259-273, 2001.

[10] Omodaka, T., Maeda, T., Miyoshi, M., Okudaira, A., Nishio, M., Miyaji, M., Mochizuki, N., Morimoto, M., Kobayashi, H., & Sasao, T., The Enormous Outburst of the 7.9km/sec Water-Maser Feature in Orion KL, *Publ. Astron. Soc. Japan*, **51**, 333-336, 1999.

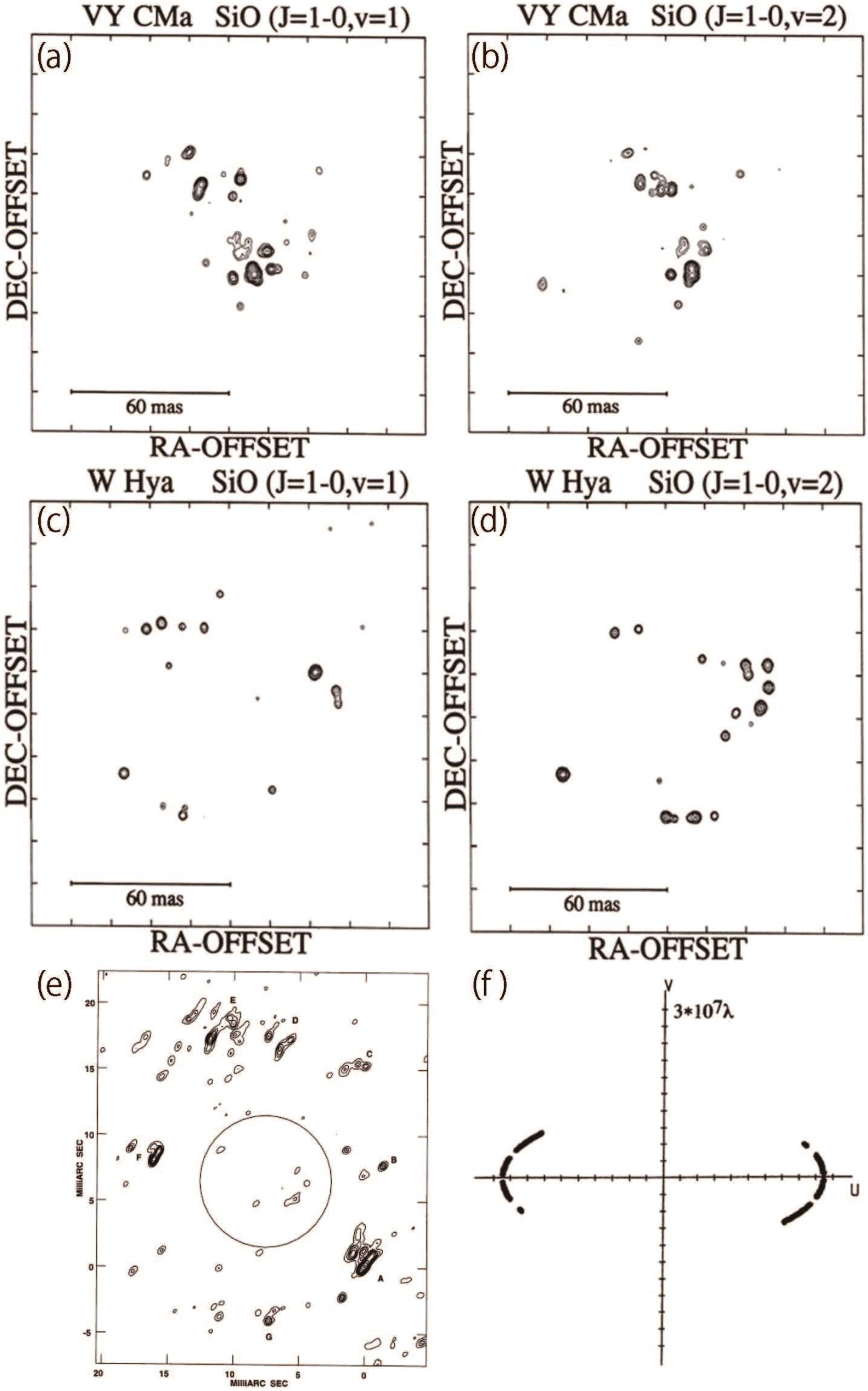

Figure 4. SiO masers observed with KNIFE. (a) VY CMa J=1-0, v=1, (b) VY CMa J=1-0, v=2, (c) W Hya J=1-0, v=1, (d) W Hya J=1-0, v=2, (e) U Her observed with VLBA [2], (f) u-v coverage of KNIFE baseline for them.

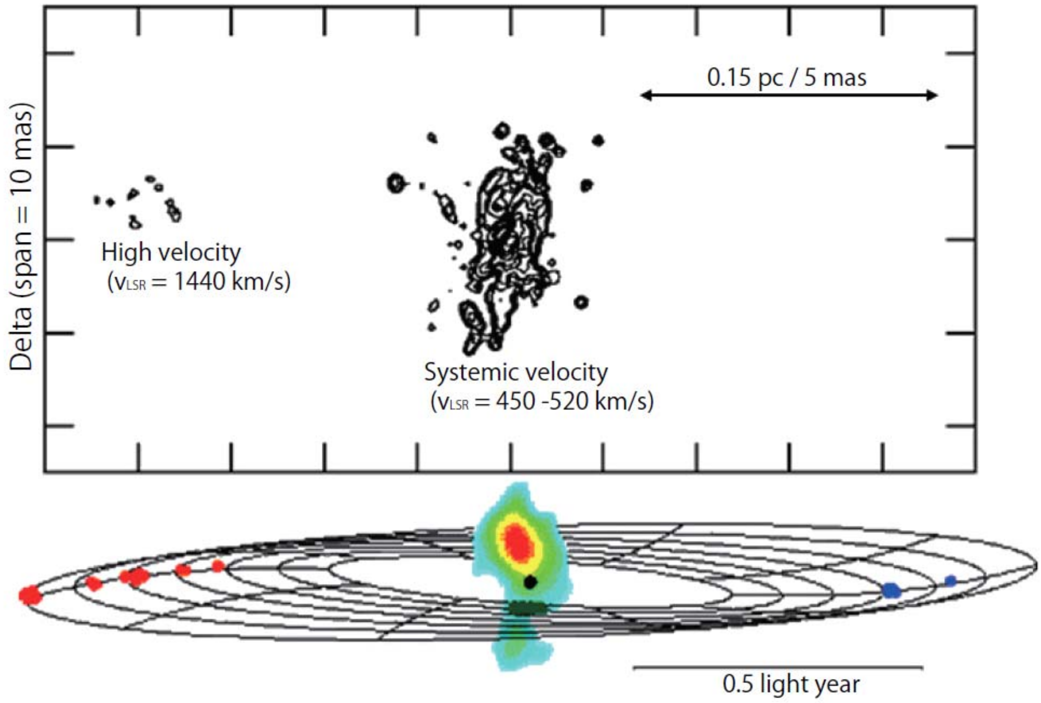

Figure 5. The oldest map of high velocity water mases in NGC 4258 observed with KNIFE in 1992 June (top panel). The image was produced in 1997. This map demonstrates that the KNIFE had the performance to clarify the structure of water mega masers in NGC 4258. The bottom panel shows the image with VLBA observations [6].

Space-Time Measurements Research Inspired by Kashima VLBI Group

Mizuhiko Hosokawa(*hosokawa@nict.go.jp*)

Principal Reseacher,
NICT, 4-2-1 Nukui-Kita-Machi, Koganei, Tokyo 194-8795, Japan

Abstract: I have done some works on the relativistic effects and precise space-time measurements, such as Time Geostationary Orbis, stellar mass measurements by using astrometric gravitational lensing, and positional fluctuation of quasars caused by gravitational lensing stars in our galaxy. Most of them are inspired by the members and legends of Kashima VLBI group. Here I introduce these memories.

1. Introduction

Kashima VLBI group is famous on the development of K-series VLBI systems and on the lots of applied research using large radio antennae. Kawajiri-san, Kawano-san, Takahashi-Fujinobu-san, and Kawaguchi-san are some of the very early member of this group, followed by many researchers, such as Yoshino-san, Takahashi Yukio-san, whom I mentioned here, and many excellent researchers. Encounters with them changed my research life. In this article, I would like to introduce how they inspired me on some of my research works.

2. Takahashi Fujinobu-san

I joined Communications Research Laboratories (CRL) in 1990. A few months after I joined CRL, I had a chance to listen to a talk on the proper time of an atomic clock onboard satellite by Takahashi Fujinobu-san. In the talk, he said his group was learning General Relativity to calculate the clock's proper time. I said to him that I can help such calculation, as in the graduate school I had learned General Relativity. Soon after hearing his talk, I tried to calculate a proper time of a space clock in the simplest circular orbit case by using Schwarzschild metric solution. Then, I found an interesting case. In a special orbit radius, the proper time of the space clock become just same as that of the clock on the Earth geoid surface. I told Fujinobu-san that result. He said he had never heard about such orbit. Then I named this orbit as "Time Geo-stationary orbit". I also thought we should write a paper on this result. However, just an idea on one orbit seems not so much for an article. So I considered a bit more and got an idea to seek orbits in the solar system whose proper times are the same as that on the Earth geoid surface in simple circular orbit approximation. After a few calculations, I found two more such orbits, one is that around Sun, a little bit inside the Earth orbit, and the other is that around Jupiter. They are shown in Fig.1. I brought these results to Fujinobu-san, had some discussion with him and presented a paper [1].

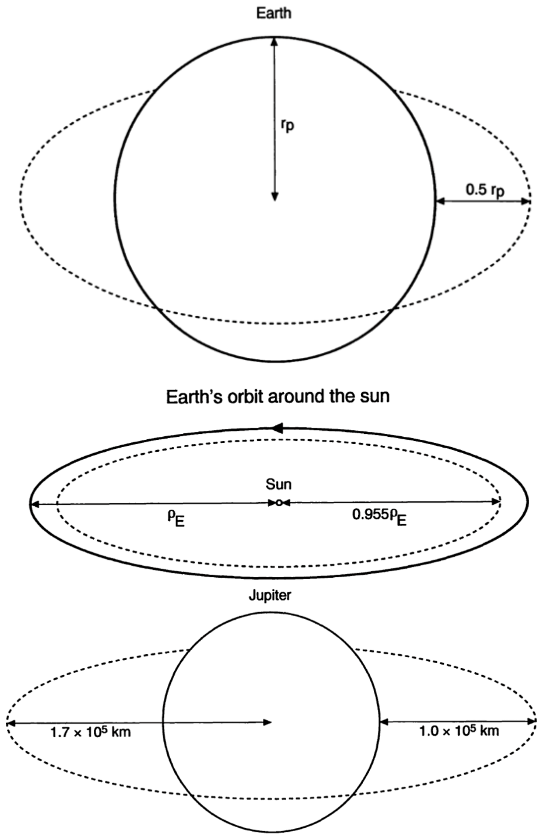

Figure 1. Time geostationary orbits around Earth, Sun and Jupiter.

3. Kawaguchi-san

This research started my join to the space-time measurements project in CRL, that include the VLBI group. In 1991 and 1992, I gave some presentation to the Japan astronomical society annual meeting on the proper time of space crafts, including Time Geostationary Orbits. At that time, some feasibility studies on space-VLBI using Japanese Engineering Test Satellite VI. I considered the relativistic effect on ETS-VI, including frequency shift with ground station. Kawaguchi-san heard my presentation and interested in that. He said that he wished to visit me to discuss on the relativistic

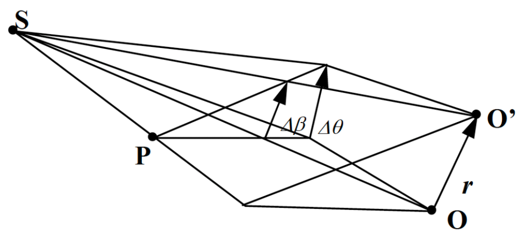

$$M = \frac{c^2\theta^2}{8G}\left(\frac{x}{\Delta\theta_x} - \frac{y}{\Delta\theta_y}\right), \qquad D = \frac{1}{2}\left(\frac{x}{\Delta\theta_x} + \frac{y}{\Delta\theta_y}\right)$$

Figure 2. Parallactic variation of gravitational lensing and measurement of stellar mass.

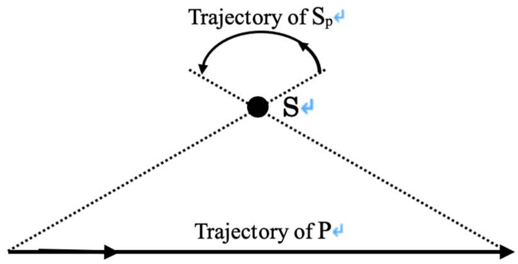

Figure 3. Apparent motion of the lensed image S caused by the proper motion of a lensing star P.

effect for space VLBI project. One or two years later, when he engaged in the HALCA space VLBI project, he visited my office. I thought that his purpose should be to hear from me the relativistic effects for satellites. However, what he said was "In order to consider the frequency transmission system between ground station and HALCA, I studied General Relativity and did some calculations. Are these results coincide with your result in ETS-VI?" Yes, he already learned General Relativity and finished the calculations. His results agreed with my calculations. I had heard Kawaguchi-san was powerful and great. At that time, I really understood that reputation.

4. Kawano-san

In late 1990 and early 1991, I had some chances to listen to the plan of VERA project, which will realize the 10 micro-arc second position measurement precision by using phase referenced VLBI technique to measure the scale of our galaxy. The key persons to this project were Sasao-san and Kawano-san. At that time, Kawano-san was already moved to National Astronomical Observatory. But I have heard Kawano-san was once a member, and a leader, of Kashima VLBI group. That made me easy to talk with Kawano-san. To hear this very ambitious plan, I was very much astonished, and thought that such high precision can be used to many other observations. An idea I got was, to measure the stellar mass using gravitational lensing effect. Fukushima-san and Ohnishi-san were interested in this idea and we started our collaboration. After many discussions, we presented a paper [2] as our first collaboration work. An illustration of the paper is shown in Fig.2. This work was thus inspired by the precision of the phase referenced VLBI technique proposed by Sasao-san, Kawano-san and many radio astronomers. I had a chance to present some work with Kawano-san. In 1997, he visited CRL with Hanada-san in NAO. He had an idea which he called inverse VLBI. He wanted Imae-san in CRL to join the system design investigation of this idea. Imae-san asked me to join this research. So I became a member of this investigation. His idea was that if we had two transmitters with atomic clocks on Mars stations, and had synchronized the clocks by two way satellite time transfer via Mars GEO satellite, we can measure many geodetic phenomena precisely by receiving the transmitters' signals with one antenna on an Earth station. After long discussions, this work was published in 1999 [3]. It is good memory for me to collaborate with one of Japanese VLBI legends.

5. Takahashi Yukio-san and ATNF

In 1993, Takahashi Yukio-san had stayed at Australian National Telescope Facility (ATNF) for one year. I envied him and wished that someday I could stay at ATNF, too. In 1996, I got a chance to apply to Japan-Australia researcher exchange program. On December 1996, an international workshop called TWAA was held in Kashima. There I gave a presentation on the fluctuation of celestial reference frame due to the gravitational lensing caused by stars in our galaxy [3]. It was one of the works under the collaboration with Fukushima-san and Ohnishi-san. In this workshop, Dr D. Jauncey at ATNF attended. After my talk, I asked Dr Jauncey that I was planning to apply Japan-Australia researcher exchange program and if I selected as the program member, I wanted ATNF to accept my stay. Dr Jauncey assured me that ATNF would accept me when the program committee selected me as the member. His words encouraged me and I was selected as the program member 1998. My stay at ATNF is first for me, but for ATNF, I was not the first visitor from CRL. So many procedures went smoothly. At the begging of my stay, I had a chance to talk with Prof. R. Ekers, the Director of ATNF at that time. Hearing a summary of what I did in CRL, he gave me an excellent suggestion. “There are three Quasars in the direction of Galactic Center, within one degree. It may be interesting to investigate the gravitational lens effect for these quasars.” I appreciated this good suggestion very much. During my stay, with the help of ATNF VLBI group, I considered on this suggestion. I also discussed with Japanese colleagues, since it was already easy to communicate with Japanese colleagues with email at that time. Applying the idea of apparent motion of the quasars induced by the stars in our galaxy, used in [4] and shown in Fig.3, we wrote a paper whose title is “Possible fluctuation of the position of Sagitarius A* relative to extragalactic radio sources” [5]. Publication of this paper was a token that my stay at ATNF was very fruitful.

6. Yoshino-san

When I joined CRL in 1990, Yoshino-san was a senior researcher of Fujinobu-san’s laboratory. In those days, when I had some question about VLBI and space-time measurements, I often asked him. And also, every time when I got some idea on space-time measurement, I told him and asked his opinion about that. His comment was, in most of the time, in a soft tone, but severe. With my idea. Many time he told me “It may be interesting. But it seems not yet so realistic.” After I came back from ATNF, I told Yoshino-san about the idea of fluctuation of Sagitarius A* relative to quasars beyond galactic center. At that time, he said that it seems much realistic idea than ever. I was very glad to hear his words, as he at last find some value in my new idea. His warm and severe comments has been giving encouragement to me.

7. Summary

Meeting with the legends and members of Kashima VLBI group has been given me lots of idea and has changed my research life very fruitfully. I deeply appreciate the group. Though 34 m antenna operation has stopped, I wish the successors of the group will open up the new research frontier.

References

[1] Hosokawa, M. and Takahashi, F., “Time-Geostationary Orbits in the Solar System”, Publ. Astron. Soc. Japan, 44, 1992, pp.159-162.

[2] Hosokawa, M., Ohnishi, K., Fukushima, T., & Takeuti, M. “Parallactic variation of gravitational lensing and measurement of stellar mass”, A&A, 278, L27, 1993.

[3] Kawano, N., Hosokawa, M., Hanada, H. & Imae, M., “Inverse VLBI method for Planetodesy”, J. of the Geodetic Society of Japan. 45, p181, 1999.

[4] Hosokawa, M., Ohnishi, K., & Fukushima, T. “Fluctuation of Extragalactic Reference Frame Due to Gravitational Lensing in Our Galaxy”, Astronomical Journal, v. 114, p. 1508, 1997.

[5] Hosokawa, M., Jauncey, D., Reynolds, J., Tzioumis, A., Ohnishi, K., & Fukushima, T. “Possible Fluctuation of the Position of Sagittarius A* Relative to Extragalactic Radio Sources”, APJL, 580, L43, 2002.

ALMA High Frequency Long Baseline Phase Correction Using Band-to-band (B2B) Phase Referencing

Yoshiharu Asaki,
Chile Observatory, National Astronomical Observatory of Japan,
Alonso de Córdova 3788, Office 61B, Vitacura, Santiago, Chile
Luke T. Maud
ESO Headquarters, Karl-Schwarzchild-Str. 2, D-85748 Garching, Germany

Abstract: In 2017, an Atacama Large Millimeter/submillimeter Array (ALMA) high-frequency long baseline campaign was organized to test image capabilities with baselines up to 16 km at submillimeter (submm) wavelengths. We investigated image qualities using ALMA receiver Bands 7, 8, 9, and 10 (285–950 GHz) by adopting band-to-band (B2B) phase referencing in which a phase calibrator is tracked at a lower frequency. In this paper we report on QSO observation experiments at Band 7 (289 GHz) and Band 8 (405 GHz) using B2B phase correction with a phase calibrator 0°.7 away observed in Band 3 (96 GHz) and Band 4 (135 GHz), respectively. The novel B2B phase referencing successfully correct the high frequency interferometer phases, achieving the angular resolutions of 15 and 11 mas at Bands 7 and 8, respectively.

1. Introduction

The Atacama Large Millimeter/submillimeter Array (ALMA) is a very powerful instrument to investigate emissions in millimeter/submillimeter waves with very high angular resolutions. With the 16 km ALMA configuration, the spatial resolutions will be 12, 7, and 5 milliarcseconds (mas) at the observing frequencies of 400, 650, and 950 GHz, respectively. The long-baseline capabilities of ALMA have been tested since ALMA early science operation started in 2011 [1–5]. ALMA has opened 16 km baseline observations to the user community up to Band 7 frequencies in Cycle 7 (≥ 0.8 mm wavelength, or ≤ 373 GHz), with the ability to regularly achieve resolutions higher than ~ 20 mas.

To achieve the highest angular resolutions with ALMA, interferometer phase stability for the 16 km baselines in high-frequency (HF) bands (Bands 8–10, or the frequency range of 385–950 GHz) is crucial. The longer the baseline, the worse the phase stability limited by atmospheric phase fluctuations, and thus the synthesized image becomes blurred [6].

To reduce the atmospheric phase fluctuations, phase referencing is a frequently adopted technique for interferometer phase correction. The general implementation of phase referencing is to frequently visit a phase calibrator, typically a bright point-like quasar (QSO), close to the target source at the same frequency. However, the flux density of a typical QSO decreases in the millimeter/submillimeter waves and the system noise increases, meaning that the integration time to achieve sufficient signal-to-noise ratio (S/N) becomes too large. This combination makes it unlikely to find a bright enough nearby phase calibrator for a randomly located target.

In order to mitigate the difficulty in finding a phase calibrator at HF, the so-called band-to-band (B2B) phase referencing provides an alternative technique, employing observations of a sufficiently close phase calibrator at a low-frequency (LF) Band [7–9].

B2B phase referencing is currently being implemented at ALMA. The motivation of the research is to verify the technical feasibility of B2B phase referencing and evaluate its performance in synthesized images with the high angular resolutions in ALMA. We report on HF long-baseline (14–16 km) image capability tests for a point source QSO J2228−0753 in Band 7 (289 GHz) and Band 8 (405 GHz) observed together with a closely located phase calibrator, J2229−0832, in Band 3 (96 GHz) and Band 4 (135 GHz), respectively, to demonstrate B2B phase referencing. In Section 2, the basic strategy of B2B phase referencing for HF long-baseline observations is mentioned. In Sections 3, we outline our ALMA B2B phase referencing observation experiments. Section 4 provides the results of the experiments and discussions. The ALMA high frequency long baseline campaign are presented in detail by other papers [10–12].

2. Basic strategy of ALMA high frequency phase correction

The main goal of the interferometer phase correction is to remove systematic phase errors due to instrumental electrical path length errors and a priori antenna position errors, atmospheric delay models over the array, and short-term atmospheric delay variations. An important delay correction produced by water vapor over each 12 m antenna is obtained by water vapor radiometers (WVR) on each antenna [13]. The WVR phase correction is always applied to the ALMA data and typically removes the majority of the water vapor delay [14], although it is somewhat dependent on the quantity of the water vapor content in the atmosphere as precipitable water vapor (PWV), the depth of the water in a column of the atmosphere to the zenith.

In 2017, HF-long baseline campaign was organized to test the submillimeter-wave (wavelength of shorter than 1.1 mm) imaging capability of ALMA using the longest baselines up to 16 km. One focus of the campaign was to extensively test the B2B phase referencing method and begin providing appropriate observing scripts and data reduction scripts. In B2B phase referencing, a close phase calibrator is observed at an LF. The LF phase of the phase calibrator is multiplied by the HF/LF ratio.

An important observation parameter in phase referencing is the switching cycle time t_{swt} that is measured by a time difference between two calibrator scans. Our experiments adopted a short switching cycle time of 20 s because HF observations may require more frequent visits to a phase calibrator to compensate for the atmospheric phase fluctuations. The ALMA antennas can quickly change their position by several degrees in a few seconds to accommodate such a quick source change.

Use of B2B phase referencing requires an additional phase correction to remove an instrumental phase offset difference between the two respective Bands. This can be achieved through a cross-band calibration, which is referred to as differential gain calibration (DGC). In the DGC, a bright QSO is observed at both the HF and LF, using frequency switching, such that the phase offset difference can be solved.

3. Experiments

We conducted the QSO observing experiments in 2017 October and November with the maximum baseline lengths of 16 and 14 km, respectively, with 40–50 12 m antennas. Overall four experiments were conducted, two in October (9th and 10th) and two in November (2nd and 3rd). We arranged B2B phase referencing experiments at two specific frequency pairs. One is at 289 GHz in Band 7 for the target with the phase calibrator observed at 96 GHz in Band 3, while the other is at 405 GHz in Band 8 for the target with the phase calibrator at 135 GHz in Band 4. There are totally two frequency sets of two observations at Bands 7 and 8.

We observed the QSO J2228−0753 as a target at the HF, while the QSO J2229−0832, with a separation angle of $0^{\circ}.7$, was observed as a phase calibrator at the LF. For DGC, we selected a very bright QSO J2253+1608 located 25° away from the target. Note that the phase offset difference measured with a DGC source is independent of the QSO location in the sky, since it is predominately determined by internal electronic phase differences between the HF and LF [10]. We switch between the HF and LF with only a ~ 2 s delay. We used DGC scans for a bandpass calibration at both the LF and HF, as well as the flux calibration.

A single observation consists of repetitions of the B2B phase referencing block for the target and phase calibrator and regular visits to the DGC block where we only switch the frequency while pointing at the DGC source. The B2B phase referencing block between the target and phase calibrator lasts 12 minutes, after which a 2.5 minute DGC block is inserted. Such a frequent insertion of the DGC block was made not only to check the DGC solution repeatability and stability but also to avoid a heavy load to the antenna control computers by a long sequence of antenna pointing changes.

Each Band amplifies two linear polarizations (X and Y) separately at each 12 m antenna. The amplified signal is split into four intermediate-frequency signals, which are referred to as basebands (BBs) with the bandwidth of 2 GHz. In our experiments, the digitized BBs were filtered out to have a 1.875 GHz bandwidth each with 128 frequency channels for two polarization pairs of XX and YY to form a spectral window. The integration time used for recording each of the four spectral windows at both the HF and the LF respectively was 1.01 s.

For the B2B phase referencing blocks, a typical science target scan length was 8 s at the HF, while the phase calibrator scan length at the LF was 6 s. For the DGC blocks, the above frequency switching sequence was adopted, and the scan length for the HF and LF DGC scan was typically 8 and 6 s, respectively. The antenna slew and/or the frequency switch are done simultaneously and take 2–3 s. The total length for the one switching cycle is ~ 20 s in both the B2B phase referencing sequence and DGC blocks.

4. Results and Discussions

4.1 Image coherence

Figure 1 shows synthesized images of the target J2228−0753 at 289 GHz (Band 7) and at 405 GHz (Band 8) after B2B phase referencing. The highest angular resolution of 14×11 mas was achieved at Band 8 with a maximum projected baseline length of ~ 13 km. To verify the image quality using B2B phase referencing, phase self-calibration was additionally conducted after B2B phase referencing. The peak flux densities of the self-calibrated images are consistent within 5% between the two epochs in both Bands 7 and 8. Since a good amplitude repeatability is achieved in the synthesis images by reducing the phase errors as much as possible, the phase self-calibrated results can be regarded as a reference.

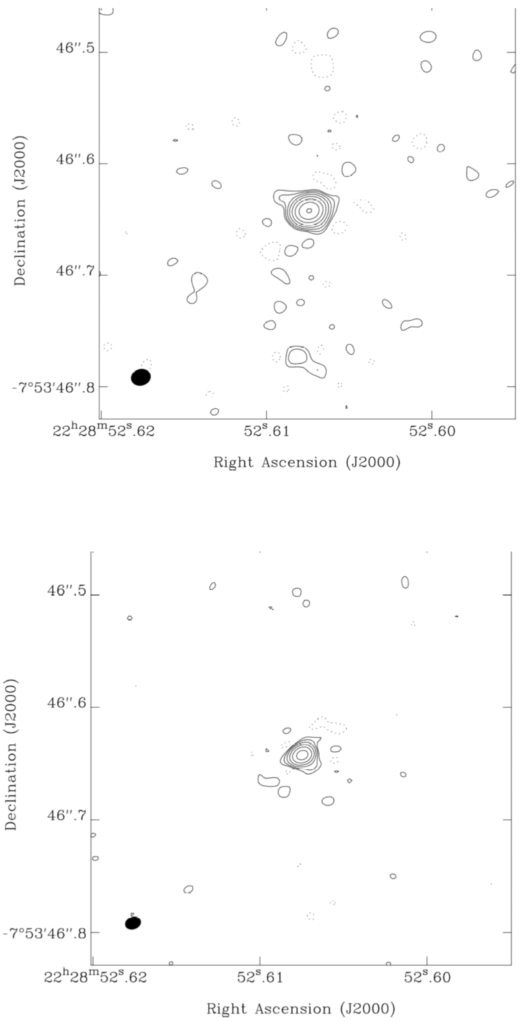

Figure 1. CLEAN images of the target J2228−0753 at Band 7 (top) and Band 8 (bottom) with B2B phase referencing. The abscissa and ordinate are R.A. and decl., respectively. The contours are drawn for a factor of -3 *(dash line), 3, 6, 12, 24, 48, 32, 64, and 128 (solid lines) multiplied by the rms noise of the images. The synthesized beam is shown in the lower left corner of each panel:* 18×15 *mas and* 14×11 *mas at Bands 7 and 8, respectively.*

One of the important indicators to evaluate the image quality is an image coherence, which is the ratio of the image peak flux density compared to the true value. We assume that the phase self-calibrated image represents the true value for each experiment. The image coherence is larger than 90% and 80% at 289 and 405 GHz, respectively, so that in our tests B2B phase referencing with a close phase calibrator and 20 s switching cycle time proves to be an effective phase correction scheme at the high frequencies.

4.2 Astrometry

Baseline vector errors cause a systematic phase error after B2B phase referencing, and thus can cause blurring of the target image. The positional shift of the target $\Delta\boldsymbol{\theta}$ (rad) due to a baseline error vector $\Delta\boldsymbol{\rho}$ (in meters) is expressed by $\boldsymbol{\rho} \cdot \Delta\boldsymbol{\theta} = \Delta\boldsymbol{\rho} \cdot (\boldsymbol{s}_{\rm t} - \boldsymbol{s}_{\rm c})$, where $\boldsymbol{\rho}$ is a baseline vector and $\boldsymbol{s}_{\rm t}$ and $\boldsymbol{s}_{\rm c}$ are unit vectors from an observer to the target and phase calibrator in the sky, respectively. In ALMA, $\Delta\rho$ is 2.5 mm for the longest baseline [15].

We investigated the target peak position in the synthesized images before self-calibration using a two-dimensional Gaussian fitting in the image plane. The averaged position of J2228−0753 for the two epochs and two Bands is $(\alpha_{\rm J2000}, \delta_{\rm J2000})$=($22^{\rm h}28^{\rm m}52^{\rm s}.607590$, $-7°53'46''.64238$) with a 1σ error of (0.24, 0.40) mas. The measured position of J2228−0753 is consistent with that in the ALMA calibrator catalogue within the quoted uncertainties. In centimeter-wave observations, J2228−0753's position is reported in the Very Long Baseline Array (VLBA) calibrator list[1] with a 1σ error of (0.10, 0.21) mas. Our B2B image position is also consistent with that in the VLBA calibrator list within 0.4 mas, less than a 20th of the Band 8 synthesized beam. For the target–phase calibrator separation of $0°.7$, $\Delta\theta$ is equivalent to $\sim$ 0.4 mas at most for a 16 km baseline, so that the obtained target position has a reasonable accuracy compared to the ALMA calibrator source catalogue and the VLBA calibrator list.

We used the ALMA data of uid://A002/Xc5802b/X5bb3, uid://A002/Xc59134/Xd47, uid://A002/Xc65717/X56f, and uid://A002/Xc660ef/X8e0 for the research. ALMA is a partnership of ESO (representing its member states), NSF (USA) and NINS (Japan), together with NRC (Canada), NSC and ASIAA (Taiwan), and KASI (Republic of Korea), in cooperation with the Republic of Chile. The Joint ALMA Observatory is operated by ESO, AUI/NRAO, and NAOJ. The authors thank to all the Joint ALMA Observatory staffs in Chile for performing the challenging HF-LBC-2017 successfully. L. T. M. was adopted as a JAO

[1] http://www.vlba.nrao.edu/astro/calib/

ALMA expert visitor during his stay. This work was supported by JSPS KAKENHI grant No. JP16K05306.

References

[1] Matsushita, S., Asaki, Y., Fomalont, E. B. et al., ALMA Long Baseline Campaigns: Phase Characteristics of Atmosphere at Long Baselines in the Millimeter and Submillimeter Wavelength, PASP, 129, 973, 035004, 2017.

[2] ALMA Partnership, Fomalont, E. B., Vlahakis, C. et al., The 2014 ALMA Long Baseline Campaign: An Overview, ApJL, 808, 1, L1, 2015.

[3] ALMA Partnership, Hunter, T. R., Kneissl, R. et al., The 2014 ALMA Long Baseline Campaign: Observations of Asteroid 3 Juno at 60 Kilometer Resolution, ApJL, 808, L2, 2015.

[4] ALMA Partnership, Brogan, C. L., Pérez, L. M. et al., The 2014 ALMA Long Baseline Campaign: First Results from High Angular Resolution Observations toward the HL Tau Region, ApJL, 808, 1, L3, 2015.

[5] ALMA Partnership, Vlahakis, C., Hunter, T. R. et al., The 2014 ALMA Long Baseline Campaign: Observations of the Strongly Lensed Submillimeter Galaxy HATLAS J090311.6+003906 at z = 3.042, ApJL, 808, L4, 2015.

[6] Carilli, C. L. & Holdaway, M. A., Tropospheric phase calibration in millimeter interferometry, RaSc, 34, pp.817-840, 1999.

[7] Asaki, Y., Shibata, K. M., Kawabe, R. et al., Phase compensation experiments with the paired antennas method 2. Millimeter-wave fringe correction using centimeter-wave reference, RaSc, 33, 5, pp.1297-1318, 1998.

[8] Rioja, M. J., Dodson, R., Jung, T.-H. et al., Verification of the Astrometric Performance of the Korean VLBI Network, Using Comparative SFPR Studies with the VLBA at 14/7 mm, AJ, 148, 84, 2014.

[9] Pérez, L. M., Lamb, J. W., Woody, D. P. et al., Atmospheric Phase Correction Using CARMA-PACS: High Angular Resolution Observations of the FU Orionis Star PP 13S*, ApJL, 724, pp.493-501, 2010.

[10] Asaki, Y., Maud, L. T., Fomalont, E. B. et al., ALMA High-frequency Long Baseline Campaign in 2017: Band-to-band Phase Referencing in Submillimeter Waves, ApJS, 247, 23, 2020.

[11] Asaki, Y., Maud, L. T., Fomalont, E. B. et al., ALMA Band-to-band Phase Referencing: Imaging Capabilities on Long Baselines and High Frequencies, AJ, 160, 59, 2020.

[12] Maud, L. T., Asaki, Y., Fomalont, E. B. et al., ALMA High-frequency Long-baseline Campaign in 2017: A Comparison of the Band-to-band and In-band Phase Calibration Techniques and Phase-calibrator Separation Angles, ApJS, 247, 23, 2020.

[13] Nikolic, B., Bolton, R. C., Graves, S. F. et al., Phase correction for ALMA with 183 GHz water vapour radiometers, A&A, 552, A104, 2013.

[14] Maud, L. T., Tilanus, R. P. J., van Kempen, T. A. et al., Phase correction for ALMA. Investigating water vapour radiometer scaling: The long-baseline science verification data case study, A&A, 605, A121, 2017.

[15] Hunter, T. R., Lucas, R., Broguiére, D. et al., Analysis of antenna position measurements and weather station network data during the ALMA long baseline campaign of 2015, 2016SPIE 9914, 99142L, 2016.

Development of a 6.5-22.5 GHz very wide band feed antenna using a new Quadruple-Ridged Antenna for the traditional radio telescopes

Yutaka Hasegawa[*1]
(*s_y.hasegawa@p.s.osakafu-u.ac.jp*),
Yasumasa Yamasaki[*1], **Hideo Ogawa**[*1], **Taiki Kawakami**[*2], **Yoshinori Yonekura**[*2], **Kimihiro Kimura**[*3], **Takuya Akahori**∗4, **Masayuki Ishino**[*5], **Yuki Kawahara**[*5]

**1 : Department of Physical Science, Graduate School of Science, Osaka Prefecture University, 1-1, Gakuen-cho, Nakaku, Sakai, Osaka 599-8531, Japan*
**2 : Ibaraki University*
**3 : ISAS/JAXA*
**4 : SKAO/NAOJ*
**5 : Kawashima Manufacturing Co.*

Abstract: We have developed a new Quadruple–Ridged Antenna to realize a very wideband feed antenna, which is highly required in astronomical and geodetic observations using radio telescopes at microwave band. This new QRA has a very low return loss of −19 dB or less over the entire 6.5–22.5 GHz, and can provide a good radiation beam pattern and sharp directivity, with small frequency dependence on its beam size, so that it can be installed into the conventional radio telescopes.

1. Introduction

One of the recent development issues in the radio telescope receiver systems is to broaden their fractional bandwidth (defined as its coverage bandwidth / its center frequency) to above 100%. Recent observation devices using the current mainstream waveguide front end, such as in ALMA, which revolutionized radio astronomy, usually have a fractional bandwidth of approximately 30%. On the other hand, in future large radio astronomy projects such as SKA (MID) and ngVLA, which will consist of hundreds of parabolic antennas, they aim at a fractional bandwidth over 100%, and will explore new science fields such as the epoch of reionization, multi-messenger astronomy including gravitational waves, and explorations of extraterrestrial life.

The problem is that such a wide bandwidth must be achieved simultaneously with high performance throughout the band. Although the conventional waveguide type feed has very high performance, it has the physical limit with a fractional bandwidth of 66% on the fundamental transmission mode. In practice, approximately 58% of the ALMA band 7+8 (275–500 GHz) is one of the maximum, and trying to broaden above 60 % is so difficult on the waveguide devices such as the Ortho–Mode Transcucer and Branch–Line Coupler. To solve this problem, antennas such as Eleven Feed[1],Quasi Self–Complementary Antenna[2], and Quadruple–Ridged Antenna (QRA)[3, 4, 5] have been developed, which can be cover more than 100% of fractional bandwidth. However, these have a very strong frequency dependence on its radiation beam pattern, and matching with the optical transmission system of the conventional (existing) telescope cannot be ensured in the entire band. In addition, its reflection amount (return loss) of the coaxial feeding unit is so large. These problems have prevented the spread of high–performance and very wideband receivers, and thus it becomes one of the development issues in recent years. In order to solve these problems, we focused on the QRA, which is considered to be compatible with the radio telescope feed, and we developed a completely new QRA model that is improved its antenna characteristics (Return Loss, Beam Pattern, Frequency Independency).

2. Features of general QRAs

Unlike other well known self–complementary wideband antennas, QRA is a super wideband waveguide antenna extending the fundamental cutoff frequency toward a lower frequency by the Ridge Waveguide. The structure of QRA is an open waveguide antenna of Quadruple-Ridged Waveguide (QR–WG) which has four ribs on four sides of a square or circular waveguide (Fig.1). In addition, a back short is provided at one end of the QR–WG, and two coaxial core wires are embedded at the resonance points as two feeding units. This feeding part is an important part that determines the reflection characteristics of QRA, and is hereafter referred as QR–Coax. The general electrical features of QRA are as follows.

1. Very broad bandwidth over 100% of the fractional bandwidth based on the wideband characteristic of QR–WG and QR–Coax.
2. Separation and transmission of V/H orthogonally polarized waves by two fundamental transmission modes that occur in QR–WG.
3. The adjustability of the radiation beam size and its pattern by optimizing the transmission mode at the apperture, such like a waveguide horn antenna.
4. The simplicity of QR–Coax with only 2 coaxial outputs.

On the other hand, most of the QRAs on the market are difficult to match with the optical transmission system of the conventional radio telescopes due to its so large beam size, and also they have so large input return loss of approximately −10 dB not adequate for a radio telescope feeder.

Thus, in this research, we designed a special QRA which solves the problem described above. The developing QRA will meet our requirements as a wideband radio telescope feed antenna.

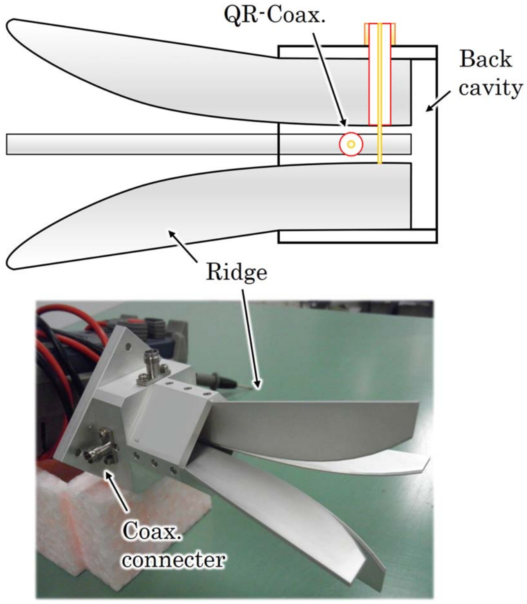

Figure 1. A schematic and photograph of the open type QRA.

3. Designing of the 6.5–22.5 GHz QRA

Fig.2 shows a schematics of the developed 6.5–22.5 GHz QRA using a 3D–FEM simulated CAD model. In this QRA designing, we adopted a waveguide horn type QRA instead of the general open type, in order to obtain the sharp beam size and perform mode matching to adjust radiation beam pattern. The circular shaped aperture dimeter is 38mm, and the distance to the back–short end (Length) is 138 mm. This is very small as a horn antenna that receives a radio wave at 6.5 GHz. The four tapered ridges, which are the characteristic structure of QRA, were shaped as an exponential curve which has less design parameters. The two pairs of taper ridge curves corresponding to each of V and H–pol were independently optimized by 3D–FEM electromagnetic simulator Ansys HFSS. In addition, the back–short end is provided with a hemispherical protrusion on the central portion of the circular waveguide as a characteristic structure of this QRA, which is called as "Plusphere back–short". This hemisphere is considered to make matching the resonance between the feeding point on QR–Coax and the back–short better in very wide band, hence the matching reduces the return loss of the QR–Coax.

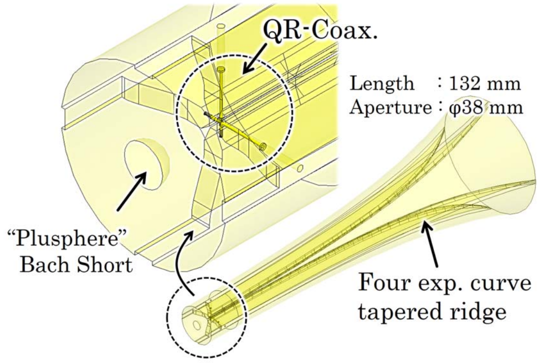

Figure 2. A schematic of the 6.5–22.5 GHz QRA HFSS simulation model.

Fig.3 shows the HFSS analysis result of the input return loss at QR–Coax of this QRA model. The Front–Port return loss which is near the apperture is approximately −19 dB in the entire band of 6.5–23 GHz, and the Rear–Port closed to the Back-Short is better than −20 dB in 6.5–22.5 GHz. These are the greatly smaller return losses than general QRAs and also enough to install into the radio observation system front–end.

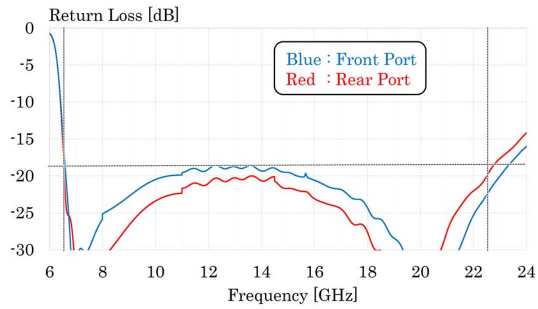

Figure 3. Calculated input return loss of the 6.5–22.5 GHz QRA.

Fig.4 shows another schematic of QRA, where in which a conical horn antenna with a wider flare angle was directly connected to the apperture of this QRA, and Fig.5 shows the simulated radiation beam pattern in the case that a signal was input to the rear port of this model. A mode matching part with an exponential curve was provided near the QRA apperture, and it was optimized to match the beam pattern and its width designed by the connected conical horn.

Accordance from Fig.5, it can be seen that the radiated beam pattern of this model has a relatively well–ordered and close to circular shaped. The beam size, i.e. the FWHM of the beam, at 6.5 GHz was approximately 28 deg in both the Az and El direction, so that the pattern was close to circular. On the other hand, though 20 deg in the Az at 22 GHz, 14 deg in the EL was relatively narrow so that the pattern was eliptical. This flattening of the beam pattern at the high frequency band is considered to be influenced by the radiation pattern of the conical horn itself, and it can be expected to be improved by optimizing the mode matching in the future. Furthermore, the beam size ratio of 3 : 1.5∼2 between 6.5 GHz and 22 GHz does not match the wavelength ratio of approximately 3.5 : 1. This is considered to be owing to the QR–WG property, which provides the wide bandwidth of QRA, and this feature can be a strong advantage in optimizing broadband optical transmission systems.

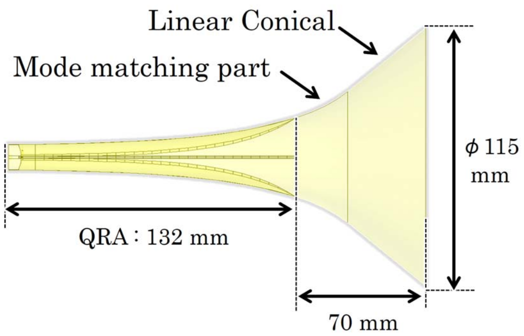

Figure 4. A schematic of the 6.5–22.5 GHz QRA with wide–flare conical WG horn.

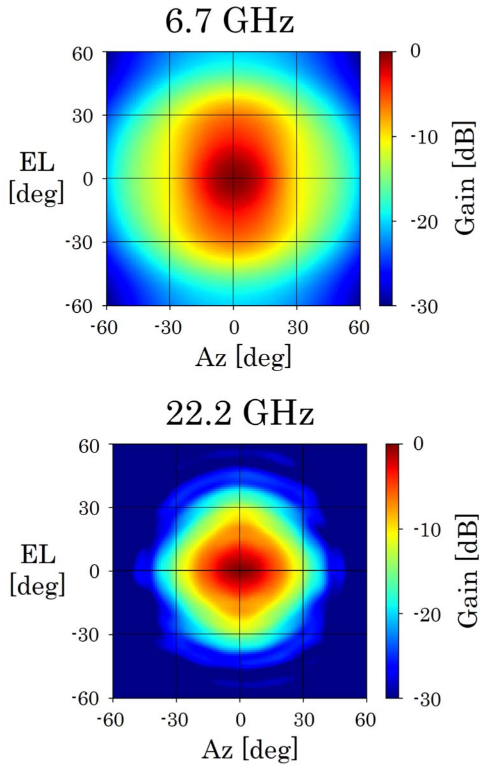

Figure 5. Calculated radiation main beam pattern of the 6.5–22.5 GHz QRA with conical horn.

4. Summary

We develop a new type Quadruple-Ridged Antenna (QRA) as a very broad band feed antenna of radio telescope. Unlike commercial products, this special QRA has a very low input return loss of under −19 dB in a very wide band of 6.5–22.5 GHz, and its radiation beam pattern is circular and relatively sharp, also these are able to modify by optimizing mode matching conical horn part. These features are very adequate as a radio telescope feed antenna including the conventional (existing) telescopes. The current status of this development is ongoing to manufacture QRA feed part called as QR–Coax, and near future we will manufacture all part of this 6.5–22.5 GHz QRA, also use it in practice to a VLBI observation.

References

[1] J. Yin, J. Yang, M. Pantaleev and L. Helldner, "The Circular Eleven Antenna: A New Decade-Bandwidth Feed for Reflector Antennas With High Aperture Efficiency," in IEEE Transactions on Antennas and Propagation, vol. 61, no. 8, pp. 3976-3984, Aug. 2013, doi: 10.1109/TAP.2013.2263275.

[2] G. Cortes-Medellin, "Novel non planar ultra wide band quasi self-complementary antenna," 2007 IEEE Antennas and Propagation Society International Symposium, Honolulu, HI, 2007, pp. 5733-5736, doi: 10.1109/APS.2007.4396853.

[3] A. Akgiray, S. Weinreb, W. A. Imbriale and C. Beaudoin, "Circular Quadruple-Ridged Flared Horn Achieving Near-Constant Beamwidth Over Multioctave Bandwidth: Design and Measurements," in IEEE Transactions on Antennas and Propagation, vol. 61, no. 3, pp. 1099-1108, March 2013, doi: 10.1109/TAP.2012.2229953.

[4] Y. Ma et al., "A 10:1 Bandwidth Cryogenic Quadruple-Ridged Flared Horn Design for Reflector Antennas in Radio Astronomy," in IEEE Access, vol. 8, pp. 81101-81115, 2020, doi: 10.1109/ACCESS.2020.2991350.

[5] A. Martellosio, M. Pasian, R. Rayet, S. Rawson and T. Bonhoure, "Wideband Cryogenic Receiver for Very Long Baseline Interferometry Applications," in IEEE Antennas and Wireless Propagation Letters, vol. 17, no. 2, pp. 275-278, Feb. 2018, doi: 10.1109/LAWP.2017.2785958.

Development of Wideband Antenna

Hideki Ujihara (*ujihara@nict.go.jp*)
Kashima Space Technology Center,
National Institute of Information and Communications Technology,
893-1 Hirai, Kashima, Ibaraki 314-8501, Japan

1. Farewell

This is the final report from Kashima about the development history for wideband antenna system. So, I would like to look back the development history of the wideband antennas briefly and say farewell to the Kashima VLBI group.

2. SIRIUS

At first, From 2009 to 2011, weak radiation measurement system was developed by the radio usage fund. The system was named SIRIUS and aimed to investigate the very weak noise from Ultra Wide Band(UWB) communication equipments or PLC, millimeter wave rader, or other communication devices. However they are weak, they can be serious interference source for radio astronomy, geodetic VLBI or some other scientific observation for weak signal detection, if their population grows. And also, their performance may be down by their own mutual interference without suitable regulation for their own noise levels. Thus our systems are aimed for so weak level of noise as -90dBm/MHz with time variation, out of the licensed bands, by detecting statistical abnormal radiation with two-element interferometer. Detection technique is based on radio astronomy, which are switching radio meter and long term averaging. The total bandwdith is from 0.8GHz to 26 GHz over, but that was divided into 3 bands because of limited bandwidth of receiver horns and IQ mixers. The low band system is designed for 0.8 GHz - 3 GHz, mid if for 3 GHz - 18 GHz, high-band is for 2GHz-26GHz. The received signal by the double-ridged horns were converted to IQ signals in video frequencies and sampled by VSSP32 VLBI sampler with USB 2.0 to be processed in the personal computers. The image is rejected by the software before several hours averaging. However narrow the bandwidth of 32 MHz which is maximal sampling rate for 8-bit in VSSP32, this wideband receiver system was the etude for the Gala-V.

3. Gala-V

Gala-V(Galapagos VLBI) project was started in 2011, which was aimed to compare the atomic clock frequencies over an inter-continental baseline with 2 small dish antennas. SNR of the total system is enhanced by the large dish of Kashima 34 m. Various wideband antennas were compared such as the Eleven feed, Open Boundary Quad-ridged Horn, Taper slot antenna, and other conventional feed horn before developing wideband antennas with narrow beam width for conventional Cassegrain antennas such as Kashima 34 m. Finally, coaxial multimode horn and axial corrugated multimode horn were selected for the candidates of the wideband feed, because they are simple and can be arranged various beam width. The Eleven feed has no room for changing its beam width, because the facing elements should keep specific angles to each other and the ground shield. Also, it needs lossy balance-unbalance transition circuit and and many LNAs. Open Boundary Quad-ridged Horn has difficulty for beam shaping. Coaxial multimode horn, named IGUANA[1], is an extension of the multimode horns for VSOP-2/ASTRO-G VLBI satellite and 6.7GHz methanol maser horns for VERA 20 m and Shanghai 25 m antenna. Axial corrugated multimode horn, named NINJA[2], is compact and has a potential for arranging the beam width. They are quite simple and easy to be manufactured by NICT. Small portable VLBI station MARBLE1 and 2 were 1.6 m and 1.5 m parabola antennas with a Open Boundary Quad-ridged Horn. They were modified into 2.4 m dish and NINJA feed to obtain 3 times better sensitivity. MARBLE1 was transported to Medicina radio observatory in the summer of 2018, and the main reflector of 34 m was well adjusted by radio holography with broad cast satellite to start the experiment. Finally the experiment shows 10^{-16} accuracy of comparison[3].

4. Next generation microwave radiometers(no name yet)

Development of a novel water vapor radiometer has been started in 2018. The will realize rapid and accurate measurement of vapor, water and oxygen in the atmosphere 15 - 60 GHz by one receiver system with a wideband feed. OMT is used to divide the signal to lower LNA(15 - 33 GHz) and higher LNA(26 - 60 GHz) because full band LNA was not found. Calibration scheme by RF switch before LNA, like SIRIUS, is not practical, because it will be increase input noise by several dB. Thus a pair of cold and hot absorbers well measured their temperatures will be set and used for reliable calibration. The 22 GHz multimode horn for VSOP-2 Bread Board Model was set on NICT Okinawa 3.7 m antenna and used in 16 - 33 GHz for an experiment to measure the water and vapor absorption in atmosphere in 2019. Wideband OMTs and feeds are developed in 2020 for 3.7 m antenna and other optics1, but experiments were postponed because of COVID-19.

5. BRAND

BRAND is the project to expand the bandwidth of European radio telescope network. Successors of IGUANA and NINJA feeds have been in evolution to 1.5 - 15.5 GHz bandwidth for secondary focus solutions2.

6. Lessons Learned

"Keep it simple, stupid" is a familiar phrase for software developers, especially Linux users. Kashima 34 m has complex receivers systems on 4 facing trollies, which push up maintenance time and cost but never guarantees position accuracy under mm. Also some feed can not be placed on the center of focus and reflectors were lost the origin of alignments. However radio holography was done with CW from a broad cast satellite, it is still unsure alignments on the reflectors and feed. Thus it is hard to guarantee the best surface by the holography over the whole band of 3 - 15 GHz, just say it is enough to the Gala-V experiments. Simply, if the symmetry of the main beam in E-cut and H-cut have been measured, alignment origin might be recovered and more efficiency was obtained. Instead of trolly system, revolving systems seemed to be reliable, or more simply tilting sub-reflector to select a horn seems to be better to make maintenance easier and better position accuracy. Also, if some feeds were combined and replaced by wideband feed, including the huge L-band horn, 34 m could have more research areas. Metabolism is important to extend the life time and applications of huge equipment like 34 m antenna, but it was not concerned to the end of 34 m.

Gala-V was named after the unique evolutions in Galapagos islands, it has several meanings and irony based on biology. What is need to survive is the variation of the food, which is the research themes and applications for the researchers. Kashima 34 m has been stick to VLBI and not so active to other studies and destroyed by a typhoon blast with slightly less speed than designated wind limit specification. I am still wondering Kashima 34 m was designed appropriately.

Acknowledgement. Next generation radiometer has been supported by JSPS KAKENHI Grant Number JP18H03828. Development of wideband feeds was supported by NAOJ Joint Development Research Grant in FY2009-FY2014 and NICT incentive fund in FY2013.

References

[1] Ujihara, H., (2016) Development of wideband feed for Kashima 34m Antenna, Radio Sci., 52, doi:10.1002/2016RS006071

[2] Ujihara, H., Takefuji, K., Sekido M., and Ichikawa R., (2018), "Development of Wideband Antennas", International Symposium on Advancing Geodesy in a Changing World, Proceedings of the IAG Scientific Assembly, Kobe, Japan, July 30 - August 4, 2017 (peer-reviewed), (10.1007/1345 2018 41).

[3] Pizzocaro, M. et al., (4th:Ujihara H.), Intercontinental comparison of optical atomic clocks through very long baseline interferometry, Nature. Physics. , doi:10.1038/s41567-020-01038-6 (2020).

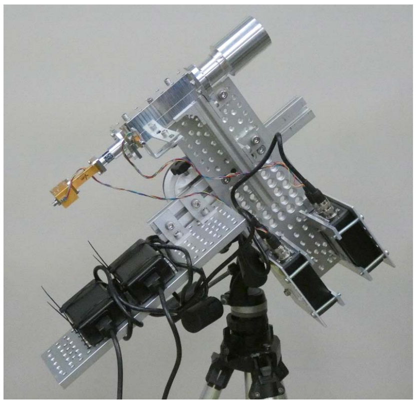

Figure 1. Wideband radiometer feed system.

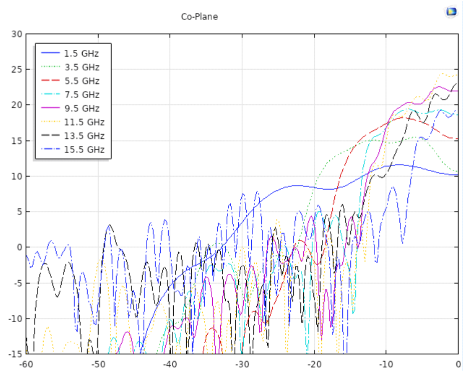

Figure 2. Simulated beam patterns of a wideband feed for BRAND.

Performance survey of superconductor filter introduced in wideband receiver for VGOS of the Ishioka VLBI station

Tomokazu Nakakuki[1]
(*nakakuki-t96nm@mlit.go.jp*),
Haruka Ueshiba[1], **Saho Matsumoto**[1],
Yu Takagi[1], **Kyonosuke Hayashi**[1],
Toru Yutsudo[1], **Katsuhiro Mori**[1],
Tomokazu Kobayashi[1], **Mamoru Sekido**[2]

1 *Geospatial Information Authority of Japan, 1 Kitasato, Tsukuba Ibaraki 305-0811, Japan*
2 *NICT Space-Time Standards Laboratory, Kashima Space Technology Center, 893-1 Hirai, Kashima Ibaraki 314-8501, Japan*

1. Introduction

The Ishioka VLBI Station operated by the Geospatial Information Authority of Japan (GSI) participates in legacy S/X sessions (2 GHz and 8 GHz band) conducted by the International VLBI Service for Geodesy and Astrometry (IVS). The Ishioka station also participates in VGOS (3-14 GHz) sessions, which is VLBI observation system promoted by IVS. Because the Ishioka station employs different receiving systems for legacy S/X sessions and VGOS broadband sessions, it is necessary to exchange receivers in order to participate in each observation. Since it takes about a week to replace and adjust the receiver, it is practically difficult to replace frequently to avoid interruption of observations. Therefore, the Ishioka station is currently regularly implementing legacy S/X sessions to maintain geodetic reference system of Japan, and is participating in VGOS sessions for several months in a year. GSI has a plan to participate in legacy S/X sessions with broadband receiver of VGOS specification in order to participate in both sessions constantly and more flexibly. Although the broadband receiver is capable to receive the 2-14 GHz frequency, the signal of S-band is seriously contaminated by strong radio frequency interference (RFI) caused by artificial radio waves around the Ishioka Station. To avoid saturation of the receiver stem by the RFI, we are currently attenuating signal below 3 GHz with applying a high-pass filter after Low-Noise-Amplifier (LNA), but there still remains a problem that the signals around 2 GHz are not available. Thus, substantial countermeasures against the RFI have been required to utilize the full-band data; 2-14 GHz. To solve the problem of the RFI, we introduced a filter that suppresses only the RFI in S-band. This report presents the results of survey and test observations to confirm the performance of the filters.

2. Characteristic survey of superconductor filter introduced in the Ishioka VLBI station

We introduced a superconductor filter to attenuate only the RFI in S-band. Because a superconductor filter has steep cut-off characteristics. In addition, cryogenic dewar of current receiver system was suitable for installation of the superconductor filter. Figure 1 shows the reflective and transmission characteristics of the filter from 1 to 15 GHz for both polarizations (H-pol: Horizontal linear, and V-pol: Vertical linear) of the introduced filter. It is designed to attenuate specific frequencies around 2 to 3 GHz. Details from 2 to 3 GHz are shown in Figure 2. It can be seen that while tiny transmission loss of 2.2-2.4 GHz used for legacy S/X session, upper and lower band to be suppressed are attenuated with sharp cutoff characteristic.

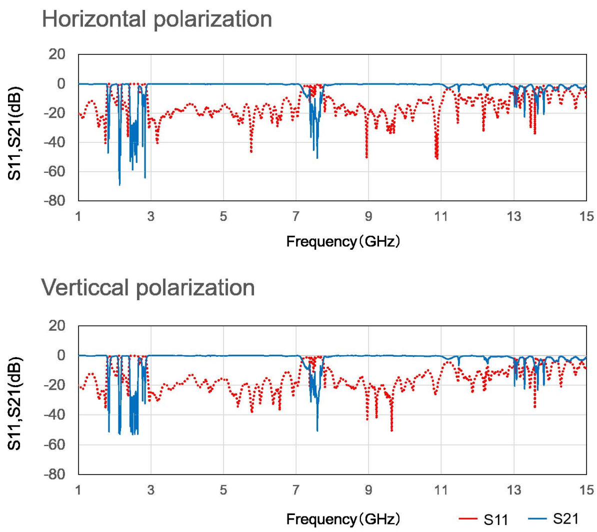

Figure 1. Green and orange curves represent the transmission and reflection characteristics of the superconductor filter, respectively. The upper panel is for the H-pol and lower panel for V-pol.

3. Detailed investigation using VLBI antenna of Ishioka

We investigated the performance of RFI attenuation after installation of superconductor filter in the cryogenic receiver system. Similary to the last year's RFI survey (Nakakuki et al., 2019), the output of LNA of broadband receiver was measured using spectrum analyzer of Agilent Technologies,

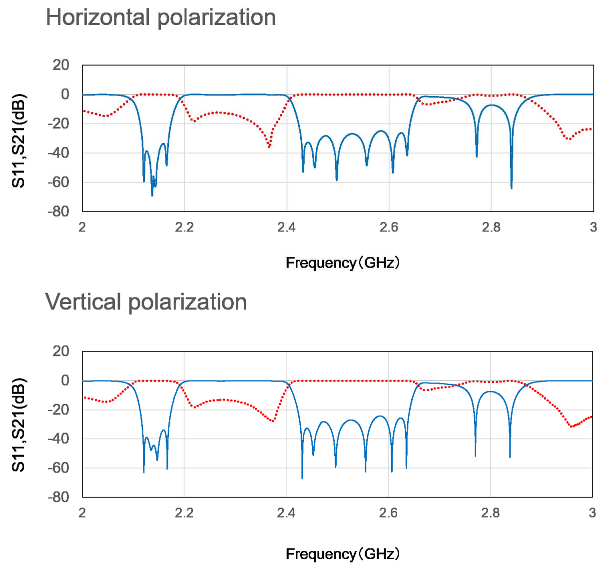

Figure 2. The same as Figure 1, but the range of frequency is 2-3 GHz.

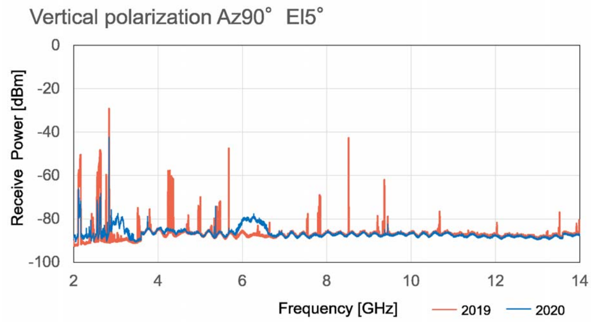

Figure 3. Receiving intensity from 2 to 14 GHz for the azimuth of 90 degrees and the elevation of 5 degrees. Blue and Orange curves represent the intensity of received signals in the surveys wtih (in 2020) and without (in 2019) superconductor filter, respectively.

Inc. We observed the spectrum while changing the elevation angle with the azimuth angle of 90 degrees (The azimuthal angle is measured in clockwise from the North. The elevation is from horizon). Figure 3 shows the received power for the frequency range from 2 to 14 GHz with an elevation angle of 5 degrees, where RFI was the strongest as in the RFI survey before the introduction of superconductor filter. As shown in this figure, both radio waves, emitted from mobile phone base station (2.1 GHz) with almost constant power and intermittently emitted radar radio waves (2.8 GHz), are attenuated. The radar power changes from time to time and it cannot always be fully attenuated. However, we suppose that is acceptable due to low

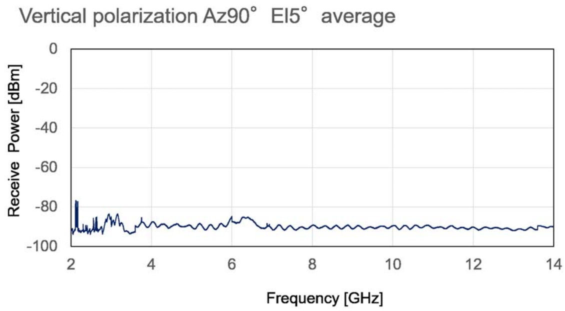

Figure 4. Averaged (100 scans) power spectrum of received signal for 2-14 GHz frequency range at Az=90 deg, El=5 deg.

time duration, and that does not appear in time averaged spectrum. (Figure 4)

4. Confirmation of fringe

Since the attenuation of the RFI was confirmed, we conducted VLBI experiment to check fringe detection. The test observations were carried out with the 11 meter antenna of the Koganei station operated by National Institute of Information and Communications Technology (NICT). Table 1 shows the conditions for the test observations. Correlation processing was carried out by NICT and GSI using K5-correlation system respectively.

Table 1. The setting of the test observations.

Obs. date	Jun. 29, 2020 5:00-6:00 (UTC)
Obs. band	S-band 6 Chs. (16MHz/1ch) X-band 10 Chs. (16MHz/1ch)
Obs.Celestial body	29 sources (Obs. time of 60 to 180 s/sources)

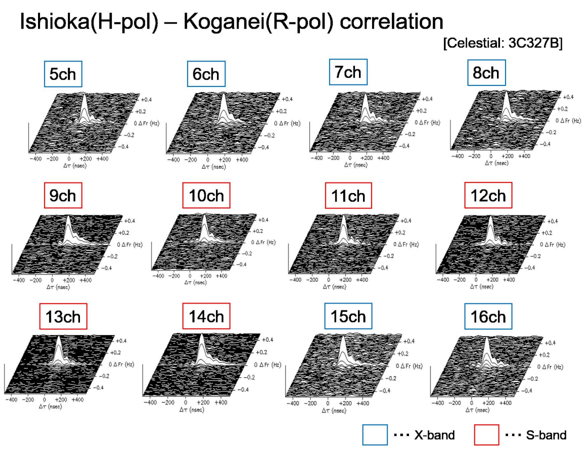

Figure 5. Correlation result of the Ishioka station (H-pol) and the Koganei station(R-pol).

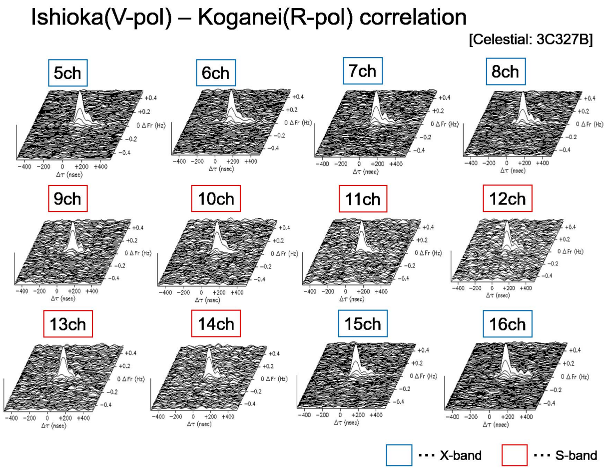

Figure 6. Correlation result of the Ishioka station (V-pol) and the Koganei station(R-pol).

5. Summary

The Ishioka station introduced superconductor filters on the broadband receiver which successfully attenuate the RFI in S-band in order to participate in legacy observations with the broadband receiver.

The investigation of the received signal revealed that the signal which caused the RFI was attenuated. In addition, conducting the test observation with the Koganei station, we confirmed that fringes were successfully detected with received signal which passed through the superconductor filter. From these results, we can say that one of the major obstacles for the observations of legacy S/X sessions with broadband receiver was resolved. For the next step to realize participation in legacy S/X sessions with broadband receiver, polarization conversion is necessary from linear to circular. We will continue effort to solve this issue.

References

[1] Nakakuki T., K. Hayashi, N. Ishikura, M. Umei, S. Matsumoto, T. Kikkawa, T. Yutsudo, H. Munekane, M. Sekido, Radio Frequency Interference research a round Ishioka VLBI Station using VGOS broadband receiver, Japan VLBI Consortium, pp.66-69,2019.

New calibration method for a radiometer without using liquid nitrogen cooled absorber

Noriyuki Kawaguchi (*kawagu.nori@nao.ac.jp*),
National Astronomical Observatory,
2-21-1 Osawa, Mitaka, Tokyo, Japan
Yuichi Chikahiro, Kenichi Harada and Kensuke Ozeki
Elecs Industry Co. Ltd.,
1-22-23 Shinsaku, Takatsu, Kawasaki, Japan

Abstract: In radio astronomy receivers and microwave radiometers, it is important to know the receiver noise temperature accurately in order to know the radiance temperature of the measurement target. Liquid nitrogen-cooled absorbers are often used to calibrate the receiver noise temperature. The liquid nitrogen-cooled absorber is a standard noise source of the most reliable, but cannot be used frequently during measurements or for calibration at various elevation angles.Therefore, we have developed a simple method for calibrating the receiver noise temperature that does not require liquid nitrogen, and here the reliability experimentally confirmed is reported.

1. Introduction

In a microwave radiometer, noise temperature of a target source is measured by so-called as a Y factor method. The noise temperature of the target, T_{tg} can be obtained from the received power ratio in the equation (1).

$$Y_1 = \frac{T_{amb} + T_r}{T_{tg} + T_r}, \tag{1}$$

where T_{amb} is ambient temperature of a non-cooled absorber or a non-reflective terminator, T_r is receiver noise temperature. The noise power amplified by the receiver is expressed as $P = kTBG$, in which k is the Boltzmann constant, B is bandwidth, G is the receiver gain, and T is noise temperature. By taking the received power ratio, the common terms, k, B, and G are removed, and only the noise temperature terms are left as shown in Equation 1. T_{amb} is easy to measure but T_r is not. In order to know the receiver noise temperature, T_r, it is necessary to measure the Y factor by the next equation, Equation 2 in advance.

$$Y_2 = \frac{T_{amb} + T_r}{T_c + T_r}, \tag{2}$$

where T_c is noise temperature of a liquid nitrogen-cooled absorber, exactly 77.364K and around 80K depending strongly to a loss of the liquid nitrogen container and slightly to barometric pressure.
The receiver noise temperature is determined by equation (2), but requires an absorber cooled in liquid nitrogen. Care must be taken when handling liquid nitrogen, and it is difficult to perform calibration work frequently. In addition, calibration at various elevation angles cannot be performed. Figure 1 shows how liquid nitrogen is filled in the container containing the absorber.

Figure 1. Liquid Niterogen filling into the absorber container at Tianma 65m site in Shanghai Astronomical Observatory

In recent years, the use cases of array antennas are increasing in the field of radio astronomy. Especially in SKA-related fields, we are promoting the introduction of 'Aperture Array' technology with the aim of improving survey speed and wide-field observation.However, it is very difficult to measure the noise temperature of the Aperture Array receiver with a built-in low noise amplifier (See Figure 2).

Figure 2. Liquid Niterogen Calibration for a large array anntena [1]

We devised a new calibration method that can measure the noise temperature of the receiver and target by a simple method without using liquid nitrogen (patent pending). In the next section theory of calibration is presented and the Section 3 experimental results are shown.

2. Theory of calibration

We introduce a microwave switch in front of a first stage amplifier, a Low Noise Amplifier, LNA, which switches between an antenna, 'Horn Antenna', a non-reflective terminator, 'Hot Terminator' , and a fully reflective terminator, 'Short Terminator' as indicated in Figure 3.

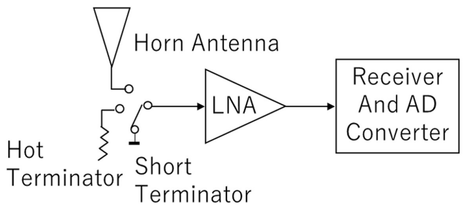

Figure 3. A schematic diagram of a new calibration system

When the switch is connected to the 'Antenna', a sky noise through the horn antenna is received, when connected to the 'Hot Terminator', ambient temperature noise is received, when connected to 'Short Terminator', a part of LNA noise is reflected and received.

Now we define a new Y-factor, a power ratio of the 'Hot' to 'Short'. expressed by an equation below.

$$Y_3 = \frac{T_{amb} + T_r}{T_{short} + T_r}, \tag{3}$$

where T_{amb} is ambient temperature to be measured by a thermometer attached on the terminator and T_{short} is a reflected LNA noise. The reflected noise temperature T_{short} is a part of the receiver noise. If we assume the factor of of the reflection is k, we can know the T_{short} as,

$$T_{short} = k \cdot T_r. \tag{4}$$

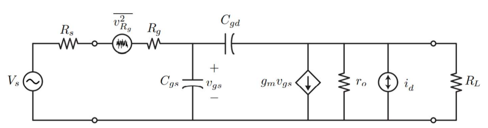

Figure 4. A simplified noise equivalent circuit of a LNA

A simplified noise equivalent circuit is shown in Figure 4. The noise generated at the 'Gate', $\overline{v_{R_g}^2}$ appeared not only on the load resistance, R_L as a receiver noise, but also on the input resistance, R_s. The coefficient, k depends on the internal parameters of the semiconductor device and needs to be measured in advance.

The parameter k is measured by placing an absorber cooled with liquid nitrogen on the horn antenna, the noise temperature of which is taken as a reference of known temperature, around 80K. The first of all, T_r is measured from a power ratio of Y_4 expressed by Equation 5 by switching 'Hot Terminator' to 'Antenna' fully covered with a cooled absorber. The power ratio can be written as

$$Y_4 = \frac{T_{term} + T_r}{T_c + T_r}. \tag{5}$$

where T_{term} is terminator temperature measured with a thermometer attached on the terminator and T_c is liquid nitrogen temperature. Both T_{term} and T_c are known so that T_r is derived from Equation 5.

In the next. switching between 'Hot' and 'Short' and the power ratio, Y_5 expressed by Equation 6 is measured. By introducing the relation, Equation 4 and the T_r measured, the k is derived..

$$Y_5 = \frac{T_{term} + T_r}{T_{short} + T_r} = \frac{T_{term} + T_r}{(k+1)T_r}, \tag{6}$$

Once k is fixed, then we can know the receiver noise temperature as

$$T_r = \frac{T_{term}}{Y_5(k+1) - 1}, \tag{7}$$

without using an absorber cooled with liquid nitrogen, only switching 'Hot' and 'Short', and we can measure the target noise temperature, T_{tg} by a power ratio of Y_1 in equation (1).

3. Experiment Results.

3.1 Receiver noise by using k

Spectra of receiver noise temperature measured with a conventional way (Hot/Cold) using a liquid nitrogen cooled absorber are compared with those measured with a new method, switching between 'Hot' and 'Short' using a k-factor in Figure 5.

Both are in good agreement and the correlation is shown in the Figure 6.

3.2 Reliability of a new calibration method

In order to test the reliability, the horn antenna is covered with an absorber cooled with liquid nitrogen, the noise temperature of which is supposed to be around 80K. Figure7 shows the test results. As a result of 10 trial tests, the mean value was 80.26K and the standard deviation was 0.25K.

In the next time, the horn antenna is covered with a non-cooled absorber, the noise temperature

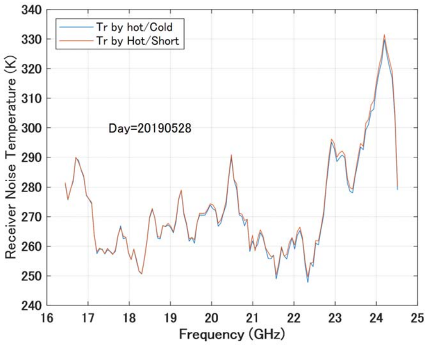

Figure 5. Receiver noise spectra measured by 'Hot'/'Cold' and 'Hot'/'Short' using 'k'

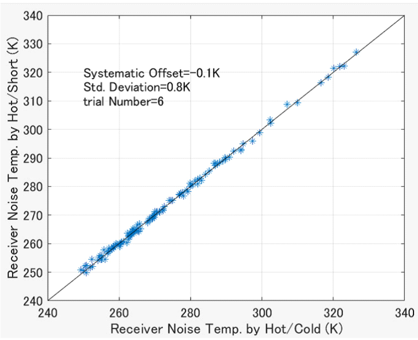

Figure 6. Receiver noise temperature measured by 'Hot'/'Cold' using liquid nitrogen cooled absorber and 'Hot'/'Short' using 'k'

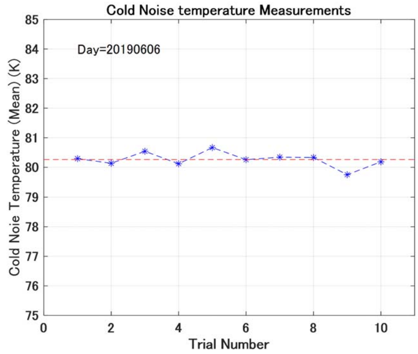

Figure 7. Cooled noise temperature of 10-times trial at a day

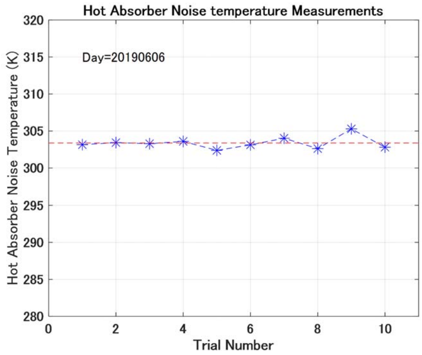

Figure 8. Terminator temperature of 10-times trials at a day

of which is supposed to be room temperature, 302K measured by a thermometer. Figure 8 shows the test results.As a result of 10 tests at room temperature of 28,9°C (302K), the average value of the noise temperature was 303.4K and the standard deviation was 0.8K. From the above test measurements for absorbers of noise temperature known, the certainty of the new calibration method was confirmed.

3.3 Long-term stability

In a previous section, results of 10-times trials on a day are reviewed. Here we present a 10-days experiment repeated same switching operation, 'Hot', 'Short', 'Antenna'. At the 'Antenna' position we covered the horn antenna with a cooled absorber and a non-cooled one, respectively.
Figure 9 shows values of k obtained on each day. the averaged value is 0.446 with the standard deviation of 0.0054. At the 6th day, it was clearly smaller than the other days. We found at the the 6-th day, the room temperature and the terminator temperature were extraordinary high by 3 to 4 degree as is shown in Figure 10. Only the day the air conditioning system was not working. Similarly, it also can be seen that the value of k tends to decrease as the temperature rises by about 0.003/deg.

In Figure 11, noise temperature of liquid nitrogen cooled absorber is shown. Blue dots indicate noise temperature when we take the k-factor calibrated on each day, the mean over the 10 days and the standard deviation are 80.30 and 0.21. Red dots indicate noise temperature when the k-factor is fixed to that calibrated in the first day, the mean and the standard deviation are 80.39 and 0.82.

In Figure 12, noise temperature of la non-cooled absorber is shown. Blue dots indicate noise temperature when we take the k-factor calibrated on each day, the mean over the 10 days and the standard deviation are 301.31 and 1.56. Red dots indicate noise temperature when the k-factor is fixed to that calibrated in the first day, the mean and the standard deviation are 302,55 and 1.44. Black dots are room temperature.

Figure 13 is receiver noise spectrum measured 10 days after using the k-factor obtained in the first day. As compared to Figure 5, the receiver noise spectrum measured in the first day and the k-factor on the day, Figure 13 shows small errors at some

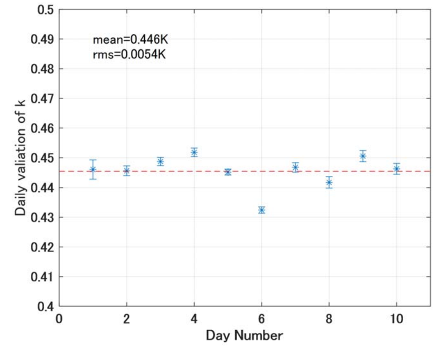

Figure 9. Stability of a parameter k over 10 days

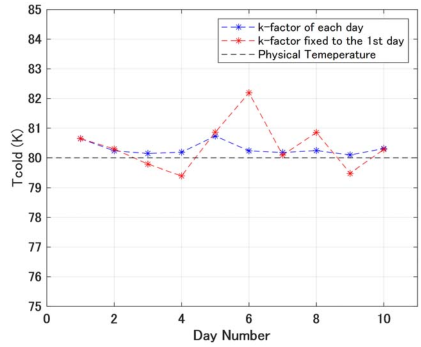

Figure 11. Stability of noise temperature of a cooled absorber over 10 days

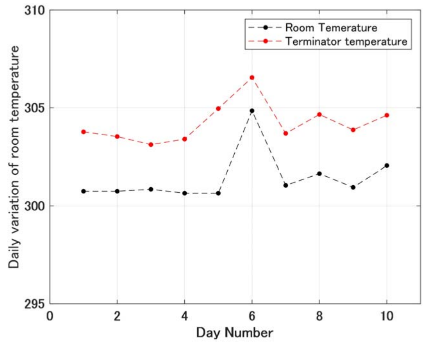

Figure 10. Room temperature variation over 10 days

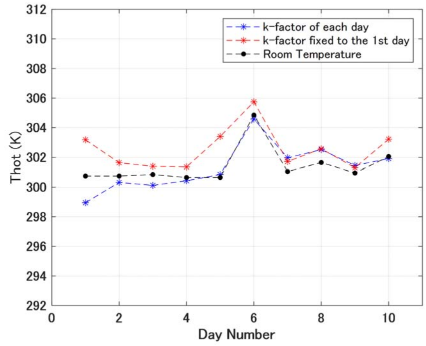

Figure 12. Stability of noise temperature of a non-cooled absorber over 10 days

frequencies, but not so large, a few kelvin in the average. We concluded the k-factor and the noise calibration without using a liquid nitrogen cooled absorber work effectively for at least 10 days, The longer test for one year is now going on at the VERA VLBI station in Iriki.

4. Summary

We successfully performed the noise calibration without using liquid nitrogen. The new calibration system is quite useful and will be introduced to a water vapor radio meter mounted on a radio telescope. This system is also effective for noise temperature calibration of array antennas. In particular, this method is indispensable for sensitivity calibration of individual array elements. Optimal beam forming will be performed in consideration of variations in the sensitivity of each array element. It is also possible to make calibration of a large array antenna without using a large container for liquid nitrogen,

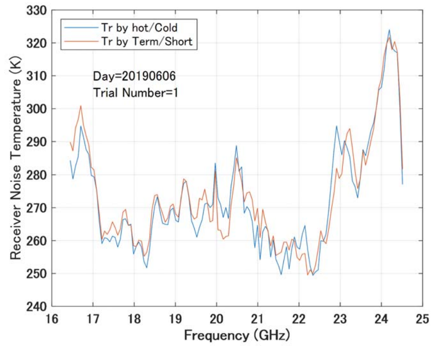

Figure 13. Receiver noise spectrum by using a k-factor calibrated in the past 10 days

5. Acknowledgments

We thanks to Dr. Akiji Nakagawa and his staff in Kagoshima University for their helps on introducing the water vapor radiometer on Iriki 20-m radio telescope. We would like to thank Dr. Takashi Maeda for his valuable advice regarding array antennas.

References

[1] A. P. Chippendale, et al., Measured Aperture-Array Noise Temperature of the Mark II Phased Array Feed for ASKAP, ISAP 2015, IEICE

Comparison of atmospheric delay models (NMF, VMF1, and VMF3) in VLBI analysis

Mamoru Sekido[1] (*sekido@nict.go.jp*) and **Monia Negusini**[2]

1 *NICT Space-Time Standards Laboratory, Kashima Space Technology Center, 893-1 Hirai, Kashima Ibaraki, Japan*
2 *Istituto Nazionale di Astrofisica/ Istituto di Radioastronomia, Via Gobetti, 101, 40129 Bologna, Italy*

Abstract: In case of VLBI observation of a long single baseline, observing antenna directions distributes in a small part of sky. Hence, accurate atmospheric delay parameter, especially anisotropic component, is difficult to estimate from VLBI data itself. Therefore, atmospheric delay model for *a priori* delay calibration is essentially important to achieve better accuracy in VLBI delay analysis of a long single baseline. We compared atmospheric delay models of NMF, VMF1, and VMF3 with broadband VLBI observation data of the Medicina - Koganei baseline. As a result of the comparison, we found that VMF3 provides the most accurate *a priori* calibration among them.

1. Introduction

We have conducted international experiments to apply VLBI for precise frequency link under the collaboration among National Institute of Information and Communications technology (NICT), Istituto Nazionale di Ricerca Metrologica (INRIM), Istituto Nazionale di Astrofisica/Istituto di Radioastronomia (INAF/IRA), and Bureau International des Poids et Mesures (BIPM). By using novel techniques in observation, signal processing, and data analysis, we successfully demonstrated the precise frequency link over intercontinental distance [1]. Moreover, geodetic performance of our system with transportable VLBI stations turned out to be comparable to standard VLBI observations made within IVS [2]. One of the key elements in the success of the experiments was calibration of atmospheric delay. Because of a long single baseline (Fig. 1), sky coverages at each antenna were limited. Hence, atmospheric delay parameters, especially anisotropic contribution, cannot be estimated accurately. In this project, we have examined atmospheric delay models provided by Niell Mapping Function (NMF) [4], Vienna Mapping Function (VMF1) [5], and its extension Vienna Mapping Function 3 (VMF3) [6]. This article describes comparison of these atmospheric delay models applied to the Medicina – Koganei baseline.

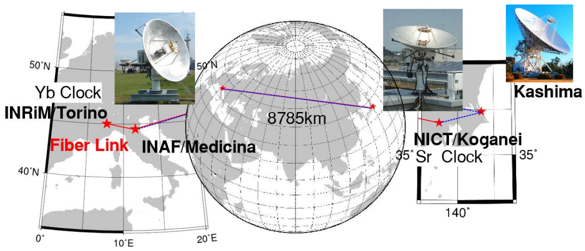

Figure 1. Medicina (Italy) and Koganei (Japan) baseline (8,785 km) was used for precise frequency link between Yb and Sr optical lattice clocks operated at INRIM and NICT, respectively.

2. Data and analysis

The VLBI data used for the comparison is the same dataset used for the frequency link[1].

Table 1 shows the list of VLBI sessions conducted between Medicina (MARBLE1) and Koganei (MARBLE2) antennas. The Kashima 34-m antenna had been participating all the sessions to form virtual delay observable via NHS scheme [2, 3], although this is not the subject here.

Fig. 2 shows the occurrence histograms of azimuthal and elevation angles at each station during these observation sessions. Corresponding histograms of standard geodetic VLBI for the period 2018-2020 are plotted for reference. Atmospheric delay contributions are parameterized in VLBI analysis by its elevation and azimuthal angles dependencies. Indeed, standard geodetic VLBI sessions are scheduled with care for sky coverage at each station. That is possible by network observation with globally distributed stations. Instead, in case of a single long baseline, observing directions are limited in a small part of sky due to mutual visibility. Atmospheric delay parameters, especially azimuth angle dependent anisotropic components, are difficult to be estimated by observation data itself as it is performed in standard geodetic VLBI analysis. Thus, we need to calibrate the atmospheric delay by *a priori* data as accurate as possible before least square analysis.

We examined NMF, VMF1, and VMF3 atmospheric delay models in data analysis with batch-Solve [7]. The NMF model is available in the Solve as bult-in model, and the atmospheric delay prediction with VMF1 and VMF3 were externally computed and stored in MK3 database as 'cable delay' data[1]. Atmospheric delay is separately modeled by the contribution of hydrostatic component referred

[1]It was because 'cable delay' data was convenient to include external calibration data in Solve analysis.

Table 1. VLBI sessions between two 2.4 m diameter antenna located at Medicina and Koganei. WRMS represents weighted root-mean-square of post-fit residuals in the baseline analysis for the NHS virtual delay.

Date	MJD	Session [h]	#Scans (Used/Total)	#Scans /hour	WRMS [ps]
5 Oct. 2018	58396	31.4	1366 / 1470	46.9	30
14 Oct. 2018	58406	28.9	1155 / 1415	49.0	32
4 Nov. 2018	58426	30.6	1452 / 1645	53.7	39
14 Nov. 2018	58436	29.0	1419 / 1539	53.1	24
24 Nov. 2018	58447	28.8	1291 / 1435	49.8	29
4 Dec. 2018	58457	29.0	1344 / 1511	52.2	33
15 Dec. 2018	58467	29.5	1379 / 1470	49.9	26
25 Dec. 2018	58477	28.9	1439 / 1501	51.8	22
15 Jan. 2019	58498	29.0	1363 / 1437	49.6	24
25 Jan. 2019	58508	30.6	1336 / 1591	56.4	26
4 Feb. 2019	58518	31.0	1342 / 1500	48.4	30
14 Feb. 2019	58528	35.8	1341 / 1585	44.3	29

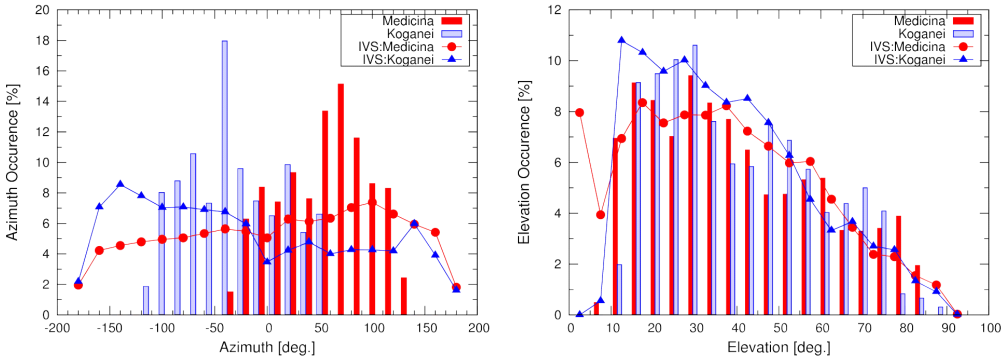

Figure 2. Occurrence of azimuthal (left) and elevation (right) angles of observation directions from each station in VLBI observation of Medicina - Koganei baseline. All the scans for twelve sessions in Table 1 are used. As a reference of standard geodetic VLBI observation, corresponding occurrence histogram data are plotted for the same stations based on the schedule files of 59 IVS sessions of R4, RDV, T2, CRF, and EURO for Medicina (●) and 91 sessions of T2, CRF, AOV, and APGS for Koganei (▲) in the period of 2018–2020.

as 'dry' and others dominated by water vapor referred as 'wet'. Each of them is parameterized by zenith delay and a factor called mapping function ($mf(\epsilon)$), which is a ratio of slant delay in the line of sight and that in zenith direction. In addition, 2-D gradient vector ($G_{\rm n}$, $G_{\rm e}$) are used in modern VLBI data analysis to represent anisotropic contribution. The Atmospheric delay model is expressed as

$$\begin{aligned}\tau_{\rm atm} &= \tau_{\rm h}^{\rm z} \cdot mf_{\rm h}(\epsilon) + \tau_{\rm w}^{\rm z} \cdot mf_{\rm w}(\epsilon) \\ &\quad + mf_{\rm g}(\epsilon) \cdot [G_{\rm n} \cdot \cos(\alpha) + G_{\rm e} \cdot \sin(\alpha)], \qquad (8)\end{aligned}$$

where ϵ and α represent elevation and azimuthal angles.

Both VMF1 and VMF3 data are based on ray tracing simulation with numerical weather data of the European Centre for Medium-Range Weather Forecasts (ECMWF). An advanced feature of VMF3 model is that provides not only mapping functions, but also gradient coefficients computed by ray tracing, and they can be used for *a priori* delay calibration. Table 2 shows the atmospheric delay models used for *a priori* delay calibration. The dry components of zenith delay were computed with ground pressure data using Saastamoinen model [9] for all the cases. The wet zenith delay parameters of both VMF1 and VMF3 and gradient coefficients of VMF3 are given by 6 hours interval, and the data are provided by the VMF data server [8]. Estimated parameters in the least

Table 2. Atmospheric delay calibration performance is compared for NMF, VMF1, and VMF3 via estimated atmospheric zenith delay parameters. Average and standard deviation computed over all the sessions listed in Table 1 are presented.

Model	Delay components	Avg. $\delta\tau^z_{\mathrm{atm}} \pm \sigma_{\mathrm{atm}}$ [ps] MARBLE1	MARBLE2
NMF	Dry	231 ± 157	237 ± 183
VMF1	Dry+Wet	-40 ± 67	0 ± 64
VMF3	Dry+Wet+Gradient	-11 ± 45	7 ± 60

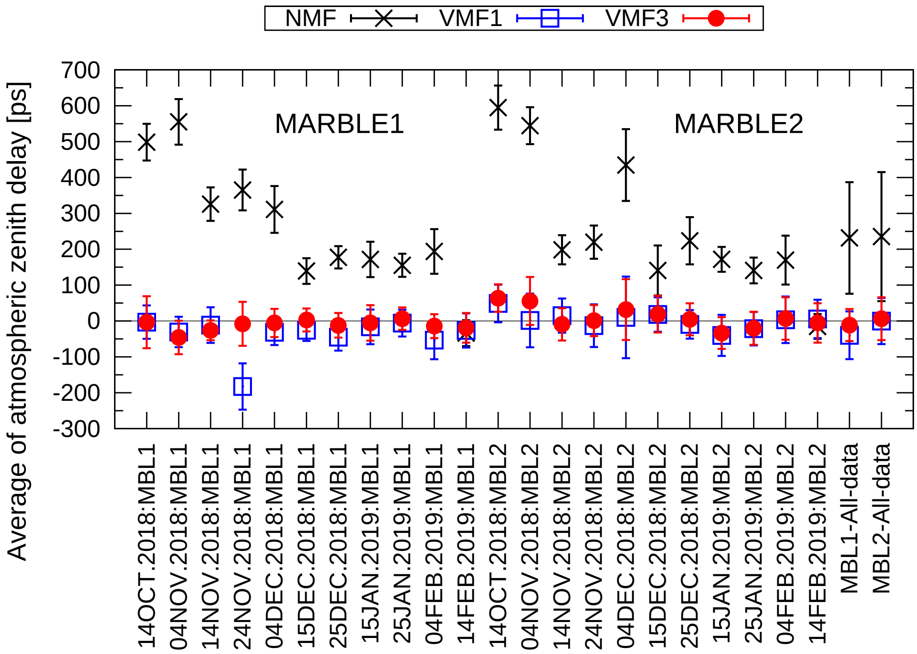

Figure 3. Estimated atmospheric zenith delay residual averaged over each session per station. Three cases of atmospheric delay calibration with NMF, VMF1 and VMF3 are compared.

square analysis are baseline vector, clock parameter (rate and offset), and zenith atmospheric delay at one-hour interval for each station.

3. Results and conclusion

Fig. 3 shows estimated atmospheric zenith delay parameters averaged over each session per station. While delay calibration using NMF results in atmospheric delay residual of hundreds of picoseconds, the remaining atmospheric delays when using VMF1 or VMF3 are of the order of tens of ps. This indicates that numerical weather model-based ray tracing technique provides very realistic atmospheric delay prediction. The smaller magnitude and lower scatter of estimated atmospheric delay (Table 2) of VMF3 compared to VMF1 can be attribute to the contribution of the gradient component of the VMF3, which represents the anisotropic property of atmosphere. This advantage of VMF3 is essentially important for the single long baseline, where estimating the atmospheric delay parameter is difficult from VLBI data itself.

Acknowledgements

We thank to all the members of collaboration team from INRIM (M. Pizzocaro, C. Clivati, D. Calonico, et al.), INAF (F. Perini, G. Maccaferri, R. Ricci, et al.), BIPM (G. Petit and J.Leute), and NICT (K. Takefuji, H. Ujihara, T. Kondo, N. Nemitz, T. Ido, et al.) for making possible this international VLBI project for precise frequency transfer. We thank J. Böhm and D. Landskron of the Vienna University of Technology (TU Wien) for providing the VMF1 and VMF3 data. We thank VLBI group of the NASA/GSFC/NVI (E. Himwich, J. Gipson, D. Gordon, et al.) for the FS9, Calc/Solve software resources that were instrumental in this project.

References

[1] Marco Pizzocaro, et al., "Intercontinental comparison of optical atomic clocks via very long baseline interferometry", Nat. Phys., 2020, doi: 10.1038/s41567-020-01038-6.

[2] Mamoru Sekido, et al., "A broadband VLBI system using transportable stations for geodesy and metrology – An alternative approach to the VGOS concept–", J. Geod., in printing, 2021.

[3] Mamoru Sekido, "'Node - HUB' Style VLBI with Broadband System", IVS NICT-TDC News. 37, pp. 22-25, 2017, URL https://www2.nict.go.jp/sts/stmg/ivstdc/news_37/pctdc_news37.pdf

[4] Arthur E. Niell, "Global mapping functions for the atmosphere delay at radio wavelengths", J. Geophys. Res. , 101, pp. 3227-3246, 1996.

[5] Johannes Böhm, Birgit Werl, and Harald Schuh, "Troposphere mapping functions for GPS and VLBI from ECMWF operational analysis data", J. Geophys. Res. 111, B02406, 2006, doi:10.1029/2005JB003629.

[6] Daniel Landskron & Johannes Böhm, "VMF3/GPT3: refined discrete and empirical troposphere mapping functions", J. Geod., 92:349-360, 2018, doi: 10.1007/s00190-017-1066-2.

[7] David Gordon, et al., "GSFC VLBI analysis center annual report", In: Armstrong KL, Baver KD, Behrend D (eds) IVS 2015+2016 Biennial Report, pp. 224-228, 2017, URL https://ivscc.gsfc.nasa.gov/publications/br2015+2016/acgsfc.pdf.

[8] VMF Data Server; editing status 2020-12-14; re3data.org - Registry of Research Data Repositories, 2020. DOI: 10.17616/R3RD2H

[9] J. Saastamoinen, "Atmospheric correction for troposphere and stratosphere in radio ranging of satellites", in *The Use of Artificial Satellites for Geodesy*, 15, 247, 1972 doi: 10.1029/GM015p0247.

HINOTORI Status Report

Hiroshi Imai (*hiroimai@km.kagoshima-u.ac.jp*), **and HINOTORI Team**

Amanogawa Galaxy Astronomy Research Center, Graduate School of Science and Engineering, Kagoshima University, 1-21-35 Korimoto, Kagoshima 890-0065, Japan

Abstract: Here we introduce our Hybrid Integration Project in Nobeyama, Triple-band Oriented (HINOTORI), which is composed of the development of a quasi-optics system capable of simultaneous signal reception in the triple bands (22, 43, 86 GHz) and the upgrade of the VLBI backend system in the Nobeyama 45 m telescope. The triple-band receiving system has been in commission since 2020 September with the expected performance. The new VLBI backend system is still being tested so as to achieve a recording rate of 32 Gbps. This report describes the specifications and the present statuses of these major HINOTORI components.

1. Introduction

Single-dish and VLBI observations that enable us to simultaneously receive and record radio signals in multiple frequency bands have demonstrated their high scientific potentials in terms of not only a higher observation efficiency but also reliable registration of radio emission maps of the multiple bands onto a common coordinate system. One of the scientific demonstrations of the simultaneous multiple band VLBI observations is presented by Yoon et al. [5], who observed circumstellar H_2O and four transitions of SiO masers in four (22, 43, 86, and 129 GHz) bands. They revealed the whole morphology of the SiO maser ring visually clarified by multiple transition maser lines and biased H_2O maser distributions with respect to the mass-losing star located at the ring center. This will shed light on the property of inhomogenous mass loss from a red supergiant.

Millimeter (especially 86 GHz) VLBI observations have made use of great benefit of such a simultaneous multiple frequency band receiving technique, which enables us to apply the band-to-band phase transfer technique and the source-frequency phase-referencing technique [1]. They shall provide solutions of fringe-phase calibration from the data in a lower frequency band (e.g., 22 GHz) to the data in higher frequency bands (e.g., 43, 86 GHz) for realizing longer coherent integration of the higher frequency band data. The special system that enables us to simultaneously observe in multiple frequency bands have been in commission at first in the Korean VLBI Network (KVN), then 40 m telescope in Yebes, Spain. Here we introduce such a system developed for the 45 m telescope of Nobeyama Radio Observatory (NRO) by HINOTORI, which has been promoted since 2016.

2. HINOTORI specification

Figure 1 shows the schematic diagram of the whole HINOTORI system.

The quasi-optics of the Nobeyama 45 m telescope enables us to select one of the receivers by inserting mirrors to and releasing them from the optics. Instead of these mirrors, the dichroic filter plate we have developed shall guide the transferred radio signals into two passes in the optics. By inserting two such filter plates, we can simultaneously receive signals in three frequency bands. The gain losses due to the filters have been measured to be $\sim$0.22 dB, causing slight increase in the system temperatures by $\sim$12 K in the 43 GHz band [3]. This gain loss is higher (1.0–1.5 dB, dependent on radio frequency) in the 86 GHz band [4]; it will be mitigated by revising the design of the filter in the future.

In order to flexibly select the multiple frequency band signals, HINOTORI shall utilize the intermediate frequency (IF) switch box operated by NRO. HINOTORI also has installed an IF selector box in which one to six out of eight IF passes are connected to the inputs of the two digital samplers OCTAD (Oyama et al., in preparation). Thus the IF signals shall be digitized in the samplers in the lower cabin of the telescope before being transferred to the VLBI backend system far away from the telescope, with keeping the instrumental excess path length stable during a VLBI observation. Moreover, HINOTORI has installed the new high speed signal recording systems, VSREC and OCTADISK2. They shall record the signals at rates of $2{\times}n$ Gbps, where $n = 2 - 24$, with a base-band-channel width of 512 MHz .

3. Status of HINOTORI development

In the first stage of HINOTORI, we have developed a system to simultaneously receive 22 and 43 GHz band signals [3]. The first light of this system was yielded in 2018 April and has been in scientific operation since 2019 December. The first user project of this system, FLASHING (Finest Legacy Acquisitions of SiO-/H_2O-maser Ignitions by Nobeyama Generation) [2] is intensively monitoring circumstellar H_2O and SiO masers for finding periodic behaviors and secular evolutions of the spectra of maser sources associated with high velocity jets so called “water fountains”.

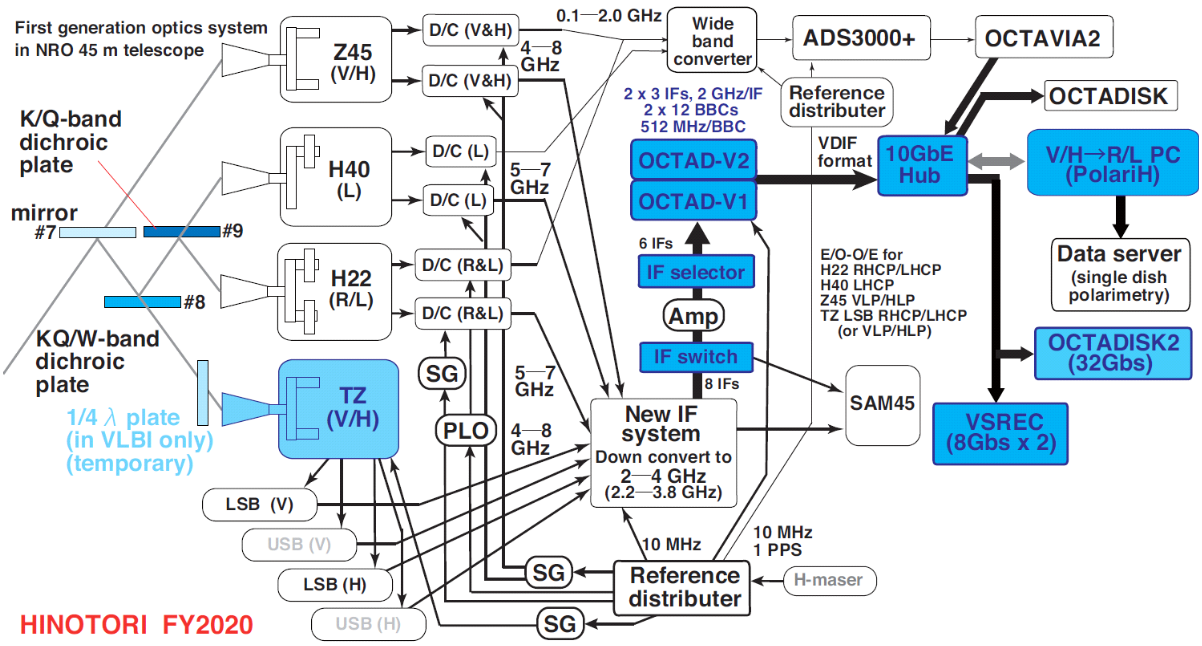

Figure 1. Overview of the HINOTORI system, which describes the signal flows in it. Color shaded components are provided from HINOTORI. Two perforated dichroic filter plates can be remotely inserted to and released from the quasi-optics so as to transfer sets of the wanted frequency band signals. Four receives named H22, H40/Z45, and TZ receive radio signals in K-band (20–25 GHz), Q-band (42.5–44.5 GHz/40–45 GHz), and W-band (80–116 GHz), respectively. The W-band signals shall be transferred to the backend in the frequency range of 85–93 GHz (lower side band) when the dichroic filter plate is inserted. In VLBI observations in the East Asia VLBI Network (EAVN) open-use program, analogue intermediate frequency (IF) signals are transferred to the digital sampler ADS3000+ (provided by NICT) for digital sampling at a rate of 4 Gbps in total in the operation building. In new VLBI experiments with the HINOTORI backend, the IF signals are digitized with two OCTAD samplers in the lower cabin of the telescope, yielding a higher recoding rate (48 Gbps in maximum) and higher fringe phase stability.

The triple-band receiving system has completed by 2020 September through re-commissioning the 80–116 GHz receiver, TZ, with its major repair in the SIS mixer and new development for its remote control system[4]. TZ itself can receive the upper and lower side band signals, while HINOTORI accepts only the latter signals due to the limited passes to the VLBI backend system and the characteristics of the dichroic filter plate. Note that TZ shall receive radio signals in two orthogonal linear polarizations. These signals will be converted to circular polarization signals by either using 1/4-λ plate or post-processing in the software that deals with cross-polarization correlation data. The latter approach is still in development.

The IF signals for VLBI were injected at proper power levels in 2020 September after installing the signal amplifiers[4]. Although the two OCTAD samplers can transfer the digitized IF signals at a rate of 48 Gbps in total, recording at the maximum data sampling rate is in a future work because recording with the new VLBI recorders is still being tested.

HINOTORI has also developed the script that enables us to operate VLBI observations remotely in the new HINOTORI system. This script shall convert a vex file provided by the principal investigator of the VLBI observation to a set of an execution file for the telescope (.start) and parameter files the frequency setup (.ndevice and .dat). It may need to be updated so as to handle a variety of the frequency setups.

4. Future perspectives

HINOTORI will reach its completion by the end of 2021 March as planed. Actualy, there still remain further development items. They are in remote IF selection, recording at the maximum sampling rate, polarization handling, and real-time spectroscopy using a PC (PolariH) for quick look and measurement of system noise temperatures in the whole baseband channels. For improving the sensitivity in the 43 GHz band by using the Z45 receiver (receiving radio signals in two orthogonal linear polarizations) in the 22/43 GHz simultane-

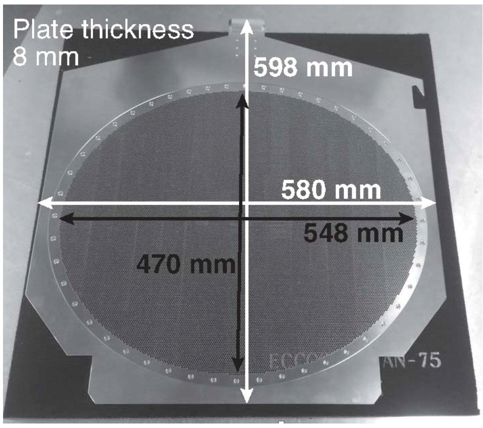

Figure 2. Perforated dichroic filter plate installed in the Nobeyama 45 m telescope. It transmits radio signals in 85–93 GHz, which shall be received with the TZ receiver, and reflects those in other frequency ranges, received with H22 and H40 receivers.

ous observation system, another dichroic filter is needed to be installed (in Mirror #7 in Figure 1).

For development of the band-to-band phase transfer technique for the 45 m telescope, a calibration scheme for differential instrumental delays among the different IF signals is an open question. Eventually we need to often observe delay calibrators. We will further need to consider to install a system to inject reference signals for such calibration.

Even with the challenging issues in the HINOTORI system, it will become a key component in future VLBI observations in the 86 GHz band in East Asia, with KVN, and the Pacific Ocean region with JCMT, Greenland Telescope (GLT), and ATCA. This style of future collaboration is under discussion over 10 years, but coming true with the beginning of scientific operation of the HINOTORI system.

Acknowledgments

HINOTORI is one of the Development Proposal projects technically supported by Nobeyama Radio Observatory (NRO) and its proposed VLBI experiments have been conducted as commissioning works approved by Mizusawa VLBI Observatory and KVN/KASI. HINOTORI has been promoted by the team members from Kagoshima University, Yamaguchi University, Osaka Prefecture University, and the National Astronomical Observatory of Japan, with the supports by KAKENHI 16H02167 and 18H03721 and that partially by Amanogwa Galaxy Astronomy Research Center, Kagoshima University. HINOTORI and EAVN have also been supported by NICT Kashima Space Research Center for installing its ADS3000+ sampler in NRO.

References

[1] Dodson, R., et al., Astrometrically registered simultaneous observations of the 22 GHz H_2O and 43 GHz SiO masers toward R Leonis Minoris using KVN and source/frequency phase referencing, AJ, 148, 97 (9 pages), 2014

[2] Imai, H., et al., FLASHING: New high-velocity H_2O masers in IRAS 18286−0959, PASJ, 72, 58 (11 pages), 2020.

[3] Okada, N., et al., Development of a 22/43-GHz-band quasi-optical perforated plate and dual-band observation system of the Nobeyama 45-m Telescope, PASJ, 71, 7 (23 pages), 2020.

[4] Tsutsumi T., in master thesis of Yamaguchi University, 2021 (in Japanese).

[5] Yoon, D.-H., et al., Astrometrically registered maps of H_2O and SiO masers toward VX Sagittarii, Nat. Comm., 9, 2534, 2018.

On-the-Fly Interferometer Experiment with the Yamaguchi Interferometer

Kenta Fujisawa[1] (*kenta@yamaguchi-u.ac.jp*), **Kotaro Niinuma**[2], **Masanori Akimoto**[2], **Hideyuki Kobayashi**[3]

(1) *The Research Institute for Time Studies, Yamaguchi University, Yoshida 1677-1, Yamaguchi-city, Yamaguchi, Japan*
(2) *Graduate School of Science and Technology, Yamaguchi University, Yoshida 1677-1, Yamaguchi-city, Yamaguchi, Japan*
(3) *National Astronomical Observatory of Japan, 2-21-1, Osawa, Mitaka, Tokyo, Japan*

Abstract: We report on an interferometric observation technique for scanning the wide field of the sky. When an interferometric observation of radio astronomy is carried out for a field wider than the beam of a single telescope, it is usual that image of each small field is synthesized in an ordinary manner and combine the images after the observation. We are studying an On-the-Fly interferometer (OtFI) observation method that continuously changes the beam position of the telescope and the phase center of the correlation process. So far, we have succeeded in scanning the beam and the center of phase, consequently detecting the fringes of multiple sources in 1 square degree field.

1. Introduction

The goal of the On-the-Fly interferometer mapping method is to detect radio sources whose positions are unknown in a wide filed of the sky with a radio interferometer. While continuously scan the beam of the element antenna in the sky (On-the-Fly), it operates as an interferometer to continuously detect radio sources in the field. Then, it will be possible to detect and list radio sources in the filed with positional accuracy of the interferometer. In this research, OtFI is tested with the Yamaguchi interferometer (YI) to demonstrate the function and the effectiveness of this new method.

2. Goals of this Experiment

The first step of this experiment is to success to scan the beam of the telescope and the phase center of the correlation processing continuously in a field of the sky. The target point of the beam and the phase center is changed at every second, and the correlation data were output every second too. When passing through a radio source with the beam/phase center, the amplitude shows the beam pattern and the phase should change linearly with time.

Since the integration time of the raw data is short, the signal-to-noise ratio of the data is low, and the amplitude information alone can provide positional accuracy equivalent to the angular resolution of the main beam. A time window is set to this data and a Fourier transform is performed, then the temporally integrated and the S / N is improved, and consequently the positions of radio sources can be estimated with the accuracy of the interferometer.

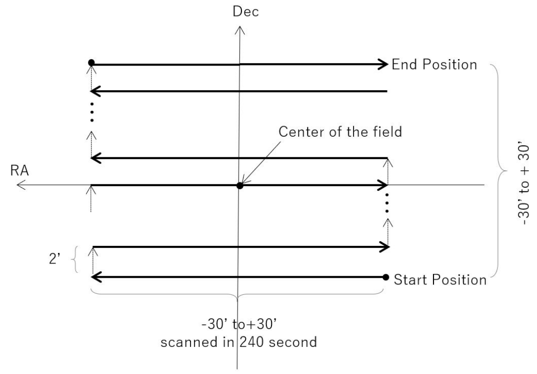

Figure 1. The scan pattern of this experiment.

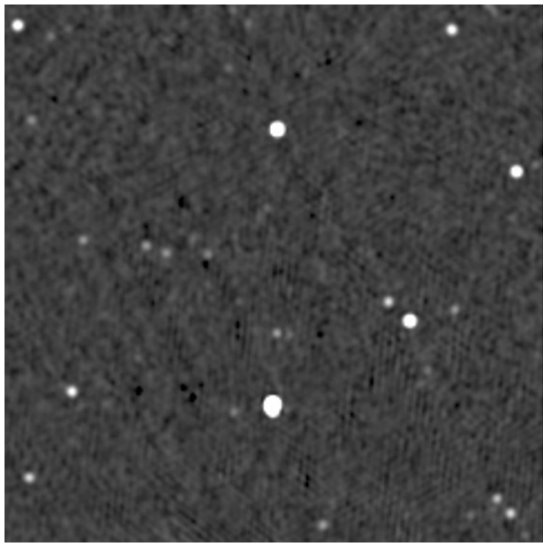

Figure 2. The observed field of 1 square degree. This image is obtained by NVSS (Condon & Kaplan 1998). The brightest source at the south part is J1055+201. The second brightest source at the north part is also detected in this experiment.

3. Experiment

The OtFI experiment with the YI is carried out on September 27, 2020, 03:00:00–05:05:00 UT. The Yamaguchi Interferometer is a single baseline interferometer with Yamaguchi 32m and Yamaguchi 34m radio telescopes. The baseline length is 109 m. The observed field is centered at RA of 10h 58m 17.9008s and Dec of +19d 51’ 50.869” (J2000.0), and ranged 1 degree both in RA and Dec. There are some radio source in this field. J1055+201 is the brightest one with flux density of 2 Jy at 1.4 GHz. The second brightest source is 400 mJy at 1.4 GHz. The scan direction is in RA with a speed of 15 arcsec/sec. The scan was repeated 30 times changing the declination of 2 arcmin at each scan. The scan pattern is shown in figure 1, and the radio image of the field by NVSS is shown in figure 2. The observing frequency is 8192-8704 MHz.

4. Results

The fringe amplitude with time is shown in figure 3. Three prominent peaks around 1800 to 2300 sec are from three scans passed over J1055+201. Two other peaks are also seen at 5660 and 5900 sec which are from the second source. The enlarged plot of this part is shown in figure 4.

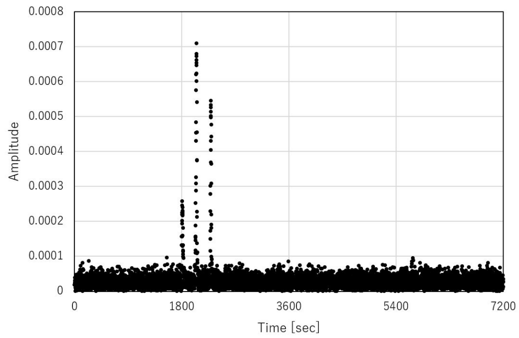

Figure 3. Fringe amplitude with time. Three prominent peaks are scans passed over J1055+201.

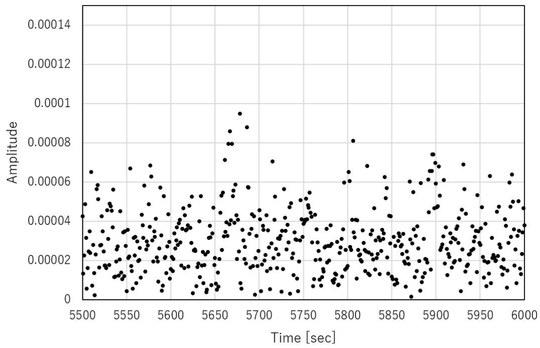

Figure 4. Enlarged plot of 5500 to 6000 sec of figure 3. Two weak peaks are seen at 5660 and 5900 sec which are scans of the second brightest source.

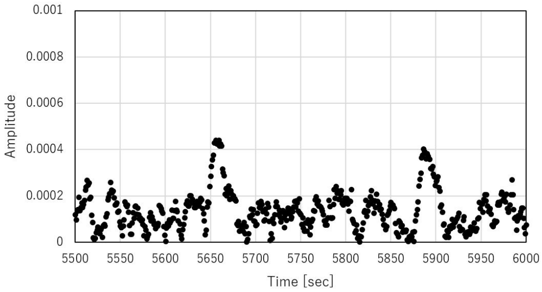

Figure 5. Time averaged plot of 5500 to 6000 sec. Two peaks are clearly seen.

Figure 5 shows the time averaged plot of the data shown in figure 4. The averaging time of 16 seconds are set to the beam (FWHM) passing time. Two peaks of the second brightest source are clearly detected. At this moment, the peak height is not correct because the averaging was performed ignoring the phase rotation. By correcting the phase rotation and performing the averaging operation, the S / N is further increased, and the third brightest source can be detected.

We have succeeded in the scan and detection of the radio sources. The next step to be carried out is (i) to derive the accurate positions of the detected sources, and (ii) to calibrate the flux density of the detected sources.

References

[1] Condon, J. J. & Kaplan, D. L. 1998, Astronomical Journal, 115, 1693

Superconducting wide-band BRF for Geodetic VLBI Observation with VGOS Radio Telescope to prevent radio frequency interference

Ken Takahashi (*ken25.takahashi@toshiba.co.jp*), **Kazuhiro Tsubosaki, Hirotaka Kamide, Hiroshi Kudou, Taro Asakura, and Masahiro Ruika**

Toshiba Hokuto Electronics Corp. Business Development Dept., New Business Planning Group,
1-1-1 Shibaura, Minato Tokyo, Japan

Abstract: The Toshiba Group has developed wide-band (1-14GHz) multi-band (hex-band) BRF using high-temperature superconductor (HTS) . The VLBI Global Observing System (VGOS) specifications require wide-band operation of the receiver from 2 to 14 GHz. And in the L-S band, there is radiofrequency interference (RFI) from other wireless systems. We confirmed that new developed BRF achieves required attenuation at each RFI frequencies and transmit response. This filter was adopted at the wide-band receiver in the Ishioka VGOS station of the Geospatial Information Authority of Japan.

1. Introduction

Superconducting filter can realize both sharp cutoff characteristics and low insertion loss. Sharp cutoff characteristics realize narrow band filter. Low insertion loss characteristics realize filters with high flexibility in design, such as BPF, BRF and those mixed Multi-band filter.

We have developed HTS filter[1] and small high-sensitibity receiver using HTS filter[2][3] for radio astronomy. In this article, we introduce the new HTS BRF for wide-band VGOS receiver(2-14 GHz).

2. Design Specification of BRF

Figure 1 outlines a block diagram of the receiver including BRFs. The cryostat with the feed horn, BRFs and cryogenic low noise amplifiers (LNAs) to be cooled down to 20 Kelvin in a vacuum chamber. The receiver is equipped with two channels for separated vertical and horizonal polarization signals. To prevent RFI effects, BRFs are placed at the input of the LNA at each channel. Yttrium barium copper oxide (YBCO) is used as a superconductor material in our work, and the HTS filter minimizes its loss at an upper boundary temperature of 77 Kelvin or lower. Under 77 Kelvin, the HTS filter can be designed according to the operating temperature.

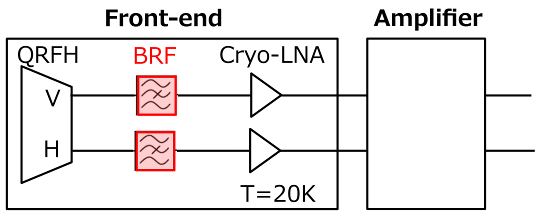

Figure 1. Schematic block diagram of receiver

Spectrum mask requirements for the BRF are indicated in figure 2. This filter has a hex-band transmit response for rejecting RFI. Required insertion loss is less than 0.5dB. The attenuation of RFI is more than 15dB, 22dB, 32dB at each RFI frequencies. In 2.1-2.4GHz, some of RFI is very close to passband. So narrow bandwidth and sharp cut off filter characteristics are needed.

Deviations in group delay of desgined filter were verified. The simulation result was confirmed to be less than 5nsec.

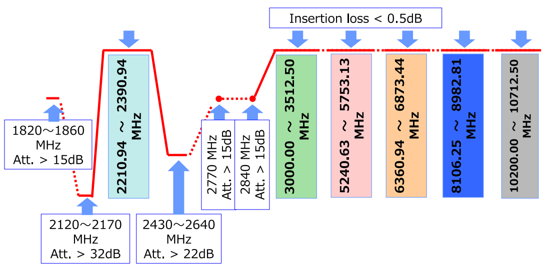

Figure 2. Spectrum mask requirements for multi-band BRF

3. Experimental Result

Figure 3 shows measured response of the BRF. Spurious response frequencies which are generated in the high frequency side (7-8GHz and 13-14GHz) are tuned to avoid observation band. Insertion loss is less than 0.5dB in the 1-10.5GHz, which satisfies required specifics. Insertion loss at high frequency edge (10.5-10.7GHz) exceeding 0.5dB and within 0.61dB, which is not the best but acceptable. At frequencies above 10GHz, unavoidable insertion loss of SMA connector, which is used input and output port of BRF module, is added to measured response.

Figure 4 shows measured detail response of rejection band(countermeasure for RFI). The attenuation of RFI is more than 15dB, 22dB, 32dB at each

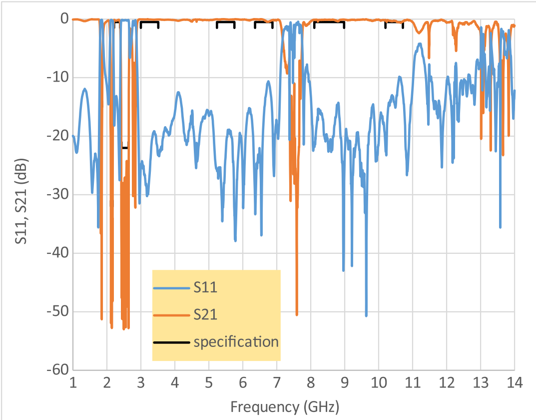

Figure 3. Measured response of BRF(1-14GHz)

RFI frequency. We confirmed that this response of rejection band satisfies required specifics.

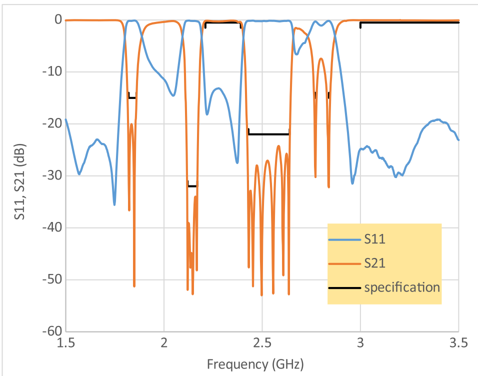

Figure 4. Detail of rejection band(countermeasure for RFI)

Figure 5 shows a photograph of BRF module. The BRF module measures approximately 79 mm long, 88 mm wide and 20 mm high. A small module size will allow it to adapt even to the existing receiver.

4. Summary

We have developed the new HTS BRF for wide-band VGOS receiver(2-14 GHz). The results of the experiments confirmed that it attenuates more than 15 dB, 22 dB, 32 dB at each RFI frequency and insertion loss of the passband is less than 0.5 dB in the 1-10.5GHz, less than 0.61 dB in the 10.5-10.7GHz. This filter is expected to realize high sensitivity wide-band VGOS receiver.

5. Acknowledgments

We would like to thank the Geospatial Information Authority of Japan for their RFI data and required filter specifications.

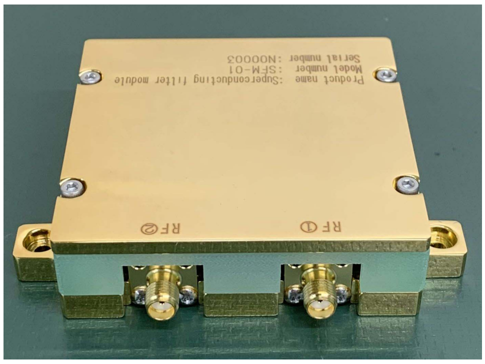

Figure 5. BRF filter module

References

[1] T. Kawaguchi, N. Shiokawa, K. Nakayama, M. Yamazaki, H. Ikeuchi, H. Kayano, Dual Band High Temperature Superconductor Filter for Radio Astronomy Station, IEICE technical report, Vol. 114, No. 11, pp. 7–10, 2014 (in Japanese).

[2] T. Kawaguchi, H. Kayano, K. Tsubosaki, H. Kamide, T. Asakura, HTS Quad-band High-sensitivity Receiver for a 4.5-m Radio Telescope, 2019 49th European Microwave Conference (EuMC), pp. 248–251, 2019.

[3] T. Kawaguchi, K. Tsubosaki, H. Kamide, T. Asakura, HTS L-S band High-sensitivity Receiver for a 20-m Cassegrain Radio Telescope, 2019 IEEE Asia-Pacific Microwave Conference (APMC), pp. 1360–1362, 2019.

Status and Future of the Mizusawa 10m Radio Telescope

Osamu Kameya (*osamu.kameya@nao.ac.jp*), **Mareki Honma, Tomoaki Oyama, Kazuyoshi Asari, Aya Yamauchi, Yu Asakura, Gen Sato, Yuki Matsukawa, Kazuya Hachisuka, Shunsaku Suzuki, Toshio Terasawa, Kazuyoshi Yamashita, VERA development group, VERA operations group, VERA maintenance group, JASMINE group, and Balloon VLBI group**
Mizusawa VLBI Observatory, National Astronomical Observatory of Japan, 2-12 Hoshigaoka-cho, Mizusawa-ku, Oshu, Iwate 023-0861, Japan
Takeshi Fukusako, and Shotaro Haruguchi
Faculty of Advanced Science and Technology, Kumamoto University, Kurokami South W2, 2-39-1, Kurokami, Kumamoto 860-8555, Japan

Abstract: The Mizusawa 10m radio telescope has been used as a VLBI station and a test bench of new VLBI and radio experiment since 1992. Now we have a plan to use it for as the downlink station of the Nano-JASMINE (Japan Astrometry Satellite Mission for INfrared Exploration) near future. We also think a new plan to use it for the low frequency observation which is below 2 GHz.

1. Introduction

The Mizusawa 10m radio telescope is 28 years old now, and it has been used for Japanese VLBI Network (J-Net) which is the first VLBI network for common use observations [1]. After the construction of the VERA (VLBI Experiment of Radio Astrometry) it has been used for many new VLBI experiments: daily observations of Sgr A* at 22 GHz [2], phase differential VLBI test observations for VERA, and RISE (Research in selenodesy; [3]). It will be used for test observations for the Balloon VLBI experiment. It has been used for single dish daily monitor observations for Orion-KL [4], and education of radio astronomy for students. It is planned to be used as the downlink station of the Nano-JASMINE (Japan Astrometry Satellite Mission for INfrared Exploration) satellite near future when the launch system becomes available [5]. Our group has a plan to use the 10m radio telescope for the low frequency observation, which is below 2 GHz, and want to use it for pulsar and fast radio burst observations.

Figure 1. The Mizusawa 10m radio telescope.

2. Recent status of the 10m radio telescope

We have installed S-band receiver, 22GHz/43GHz receiver on the telescope, and we can observe both S-band and the other one band simultaneously. While the budget for Mizusawa VLBI Observatory has been reduced from last year, there is no prospect of operating costs from this year onward. Therefore, we are considering operation and development with compensation from individual research expenses, scientific research expenses, and others. We are also responding with the help of everyone involved. Over the past year, the 10m radio telescope has had some problems due to its aging. That is, the air conditioning in the receiver room was stopped, the LAN in the receiver room was malfunctioning, the K-band compressor was stopped, the performance of the optical transmission device was deteriorated, the OS of the antenna drive computer (Windows7) should be updated, and the S band reception performance was deteriorated. These have been resolved individually.

3. Current status and future of low-frequency receivers

The purpose of the low-frequency observations is securing radio telescopes capable of low-frequency

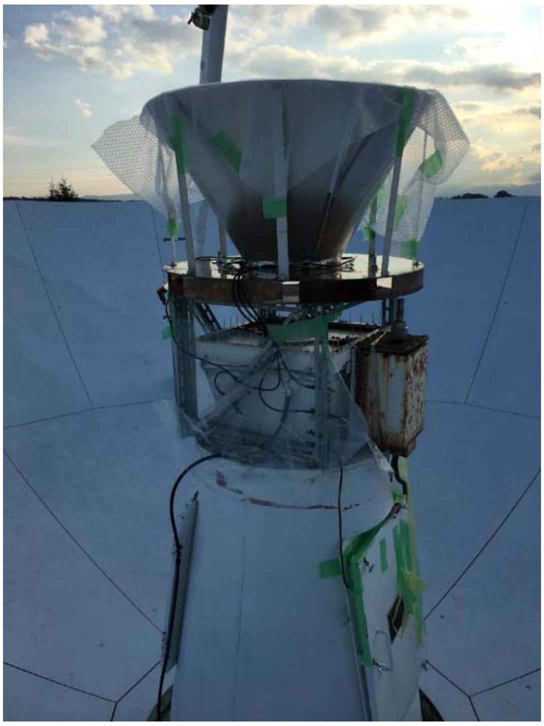

Figure 2. The L-band system.

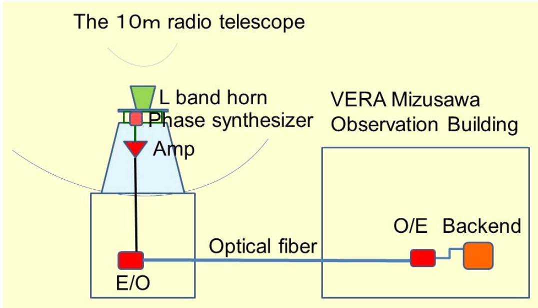

Figure 3. Schematics of the L-band system

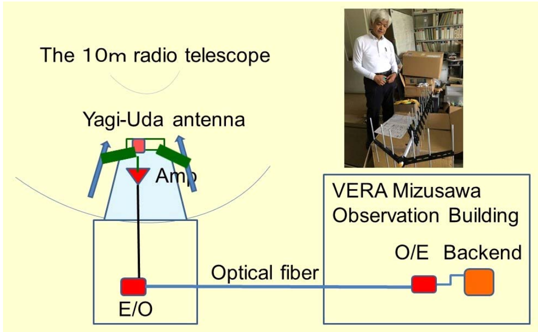

Figure 4. Schematics of the lower frequency system.

observation of pulsars and transient sources with an eye on SKA, etc. We consider the following three future items: (1) Improvement of the existing system in the S-band, (2) Development of L-band system, (3) Aiming for the lower frequencies.

3.1 Improvement of the existing system in the S-band

The purpose is to enable observation of the giant pulse of the crab pulsar with high temporal resolution. Therefore, RF is sent to the observation building using E/O and O/E without using the existing down converter, and RF is recorded directly in the observation building. Currently, we are re-inspecting the system that has already been installed. Since the performance of the horn deteriorated due to rust, the rust was removed to improve it.

3.2 Development of L-band system

This system was developed by Prof. Fukusako and his student in Kumamoto University. The purpose is to study an L band receiving system for this telescope. Initially, we considered 1.4 GHz to 1.6 GHz, but changed it to 1.05 GHz to 1.45 GHz in consideration of the FIRST frequency. For use in this radio telescope, we considered improving gain and reducing cross-polarization [6]. We will show the schematics of the L-band system. L-band RF signal comes to the observation building by using an E/O and O/E and optical fiber line and directly sampled by backends. The schematics of the L-band system is shown in Fig.3. At present, interference is strong, and the performance of the receiver system is not sufficient. It is necessary to optimize the level and improve the horn position. In the future, when a good-performance L-band system is constructed on this telescope, simultaneous observation with a large-diameter radio telescope such as FAST would be expected.

3.3 Aiming for the lower frequencies

Observations of the frequency lower than 650MHz will be challenging and very interesting because many pulsars have strong emission at such low frequency. In Japan, Iidate station of Tohoku University can observe such low frequency. If we make the low frequency system on the 10m radio telescope, we can conduct some simultaneous observations with the Iidate and the other low frequency stations. We have planned to install such low frequency using Yagi-Uda antennas. The planned schematics is shown in Fig. 4.

4. Summary

The Mizusawa 10m radio telescope has been used as a VLBI station and a test bench of new VLBI and radio experiment for more than 28 years. This telescope is planned to be the down link station of the Nano-JASMINE satellite near future. We also have plans to use this telescope at the lower frequency which is lower than 2 GHz including L-band and lower than 650MHz.

References

[1] Omodaka, T., O. Kameya, M. Miyoshi, T. Miyaji, T. Sasao, T. Kondo, Y. Koyama, J. Nakajima, M. Sekido, E. Kawai, H. Osaki, H. Okubo, M. Imae, Y. Takahashi, N. Kurihara, H. Takaba, T. Iwata, N. Kawaguchi, K. Iwadate, H. Kobayashi, K. Shibata, S. Kaneko, Y. Murata, and H. Imai, Operations and Results of J-Net (Japanese Domestic VLBI Network), Journal of the Communications Research Laboratory, Vol.48, No.1, 23-29, 2001.

[2] Kameya, O., M. Tsuboi, Y. Asaki, Y. Yonekura, Y. Miyamoto, H. Kaneko, M. Seta, N. Nakai, M. Miyoshi, H. Takaba, K. Wakamatsu, Y. Fukuzaki, T. Morimitsu, M. Sekido, 22 GHz MONITORING OF SGR A* DURING THE G2 PERI-CENTER PASSING WITH THE JAPANESE VLBI NETWORK, Publications of The Korean Astronomical Society, vol. 30, issue 2, pp. 649-650, 2015.

[3] Hanada, H., T. Iwata, N. Namiki, N. Kawano, S. Sasaki, K. Matsumoto, H. Noda, S. Tsuruta, K. Asari, T. Ishikawa, F. Kikuchi, Q. Liu, S. Goosens, Y. Ishihara, N. Petrova, Y. Harada, K. Shibata, K. Iwadate, O. Kameya, Y. Tamura, X. Hong, J. Ping, Y. Ali, S. Ellingsen, and W. Schluter, The Exploration of Lunar Gravity by VLBI Observations of SELENE (Kaguya), Trans. JSASS Space Tech. Japan, Vol. 7, pp.Tk 1-Tk 5, 2009.

[4] Horiuchi, S. and O. Kameya, Highly polarized emission from the bursting water maser in Orion-KL, Publ. Astron. Soc. Japan, 52, 545-550, 2000.

[5] Gouda, N., T. Yano, Y. Yamada,Y. Kobayashi, T. Tsujimoto, and the JASMINE Working Group, " Japan Astrometry Satellite Mission for Infrared Exploration (JASMINE), " ESA RSSD (Research and Scientific Support Department), 2004, URL: `http://www.rssd.esa.int/SA/GAIA/docs/Gaia_2004_Proceedings/Gaia_2004_Proceedings_77.pdf`

[6] Haruguchi, S., Dual-polarized Horn Antenna with Low-profile Structure, Master 's thesis, Kumamoto University, 2019.

- News - News - News - News -

Kashima 34-m Antenna Closing Ceremony

Mamoru Sekido (*sekido@nict.go.jp*)

*NICT Space-Time Standards Laboratory,
Kashima Space Technology Center,
893-1 Hirai, Kashima Ibaraki, Japan*

1. A brief hisotory of Kashima 34-m antenna and VLBI researh

Kashima 34-m antenna closing ceremony was held on 3rd Oct. 2020, which was about one year after the stop of operation. Elevation drive mechanics and part of reflector structure was damaged by strong typhoon Faxai attacked to Kashima on 9th Sept. 2019. That was decided to be dismantled in 2020, and that work is underway now (as of January 2021). History of Kashima Space Technology Center of NICT goes back to 1964. The Kashima branch of Radio Research Laboratory (RRL; Name has been changed to CRL in 1988 and to NICT in 2001) was established in 1964 for technology development of satellite communication and broadcast. Steerable parabola antennas of 30 m diameter (1964) and 26 m antenna (1968) were built for technology development in that field. Television picture of the Olympic games held in Tokyo 1964 was transferred by satellite link from Kashima to Ponit Mugu station of California in USA, then broadcasted in the USA and Europe. The 1960s was era of historical big discoveries in radio astronomy, such as quasar (1963), Cosmic microwave background (1965), and pulsar (1967). Radio astronomers in Japan focused on these antennas and had visited Kashima to use these high gain parabola antennas for radio astronomical observations, and then collaboration has started between RRL and National Astronomical Observatory. In 1971, VLBI research at Kashima has started by an offer of collaboration about VLBI proposed from NASA Goddard Space Flight Center (GSFC). A VLBI group was formed in Kashima in 1975, and the first domestic VLBI experiment was successfully performed in 1977. Since then, Kashima 26-m antenna (Fig. 1) joined international geodetic VLBI experiments conducted by NASA. These experiments resulted the detection of contraction of baseline length between Kashima and Kauai, and it provided a proof of plate tectonics. Based on the great success of geodetic VLBI with 26-m antenna, Kashima VLBI group has made big progress. The Kashima 34-m antenna was built in 1988 as one of radio telescopes of Western Pacific VLBI Network (WPVN) project, which is targeting measurement of plate motions around the Japan Islands.

Not limited to geodetic measurement of pacific plate motion, Kashima 34-m antenna has made critical role in many technology developments. Three generations (K3, K4, and K5) of VLBI observation systems were developed in Kashima, and they have been used as standard geodetic VLBI system in Japan. Our activity as the IVS technology development center has been published by this IVS NICT-TDC news (`https://www2.nict.go.jp/sts/stmg/ivstdc/news-index.html`).

2. Kashima 34-m antenna closing ceremony

Closing ceremony of the Kashima 34-m VLBI station was held as the memorial event on 3rd Oct. 2020. Originally it was planned in the end of April 2020 having about 200 attendees including invited individuals and citizens. However, due to COVID-19, that was postponed to October and it was changed to hybrid form with small number of attendee and online broadcast to the public via YouTube (https://youtu.be/kXaWl3zDP8g). The ceremony started from the opening address by the president of NICT. Then, video messages of invited participants were showed. Although, the invited guests (Prof. Axel Nothnagel as the chair of IVS directing board, Prof. Zhiqiang Shen as director of Shanghai Astronomical Observatory, Ed. W. Himwich from NASA/GSFC, Prof. Hideyuki Kobayashi of NAOJ, and Satoshi Fujiwara as director of GSI/Space Geodesy Division) could not attend due to the disaster, they contributed the ceremony by kindly sending video or letter messages. Following to the ceremony, public lectures were given by Mizuhiko Hosokawa (a former member of directors' board of NICT), Prof. Kosuke Heki (Hokkaido Univ.) and Takashi Takahashi (director of Kashima Space Technology Center (KSTC)). Hosokawa talked about achievement of Kashima 34-m VLBI station in the field of geodesy and astronomy. Prof. Heki used to be a member of Kashima VLBI group, and he gave lecture on recent results of space geodesy. Takahashi talked on past and future of satellite communication technology in relation with KSTC. More than 13 old VLBIers, who used to be worked at Kashima, got together for the ceremony and we said goodbye to the Kashima 34-m antenna. The video of the whole event is still available from YouTube (https://youtu.be/kXaWl3zDP8g).

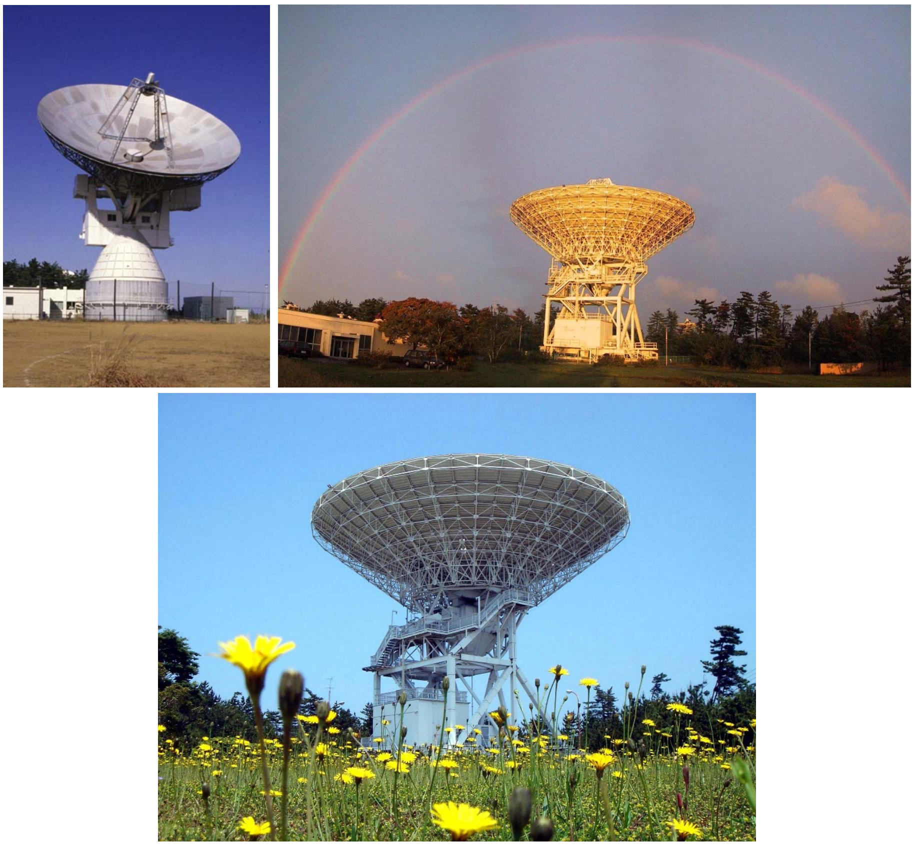

Figure 1. Top left: Kashima 26-m antenna (1968–2002) played an important role in the history of geodetic VLBI in Japan. Kashima 34-m antenna was built on the success of this antenna. Top right: Raibow above the antenna on 12th Nov. 2001. Bottom: Kashima 34-m antenna on 5th Jun. 2006.

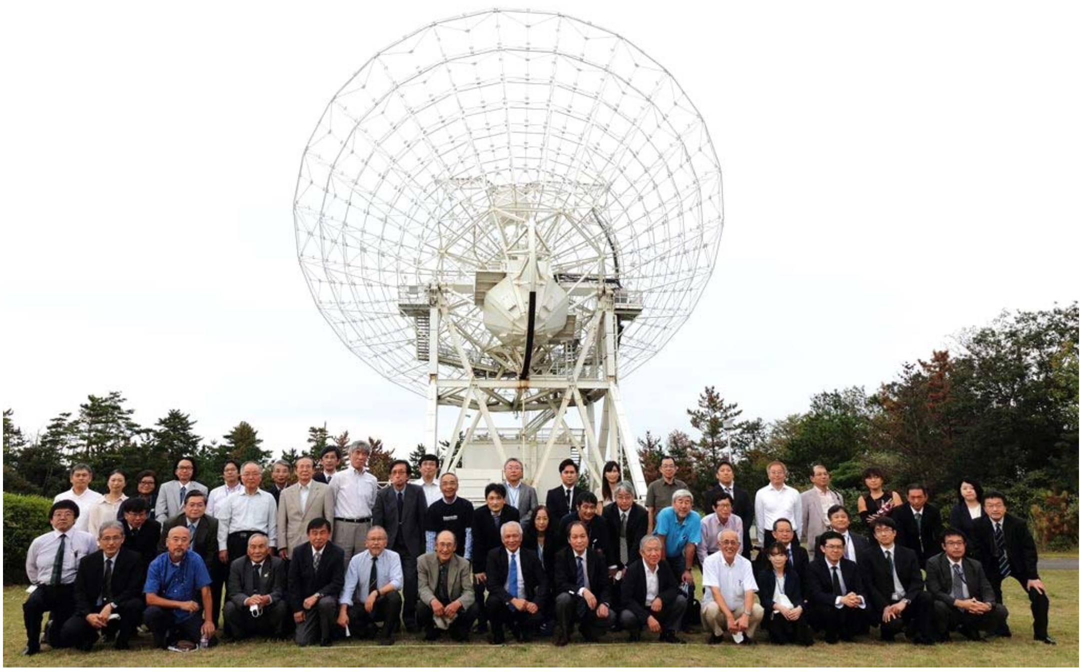

Figure 2. Group photo of the attendees to the ceremony on 3rd Oct. 2020.


©Ujihara

"IVS NICT Technology Development Center News" (IVS NICT-TDC News) published by the National Institute of Information and Communications Technology (NICT) (former the Communications Research Laboratory (CRL)) is the continuation of "IVS CRL Technology Development Center News" (IVS CRL-TDC News). (On April 1, 2004, Communications Research Laboratory (CRL) and Telecommunications Advancement Organization of JAPAN (TAO) were reorganized as "National Institute of Information and Communications Technology (NICT)".)

VLBI Technology Development Center (TDC) at NICT is supposed

1) to develop new observation techniques and new systems for advanced Earth's rotation observations by VLBI and other space techniques,
2) to promote research in Earth rotation using VLBI,
3) to distribute new VLBI technology,
4) to contribute the standardization of VLBI interface, and
5) to deploy the real-time VLBI technique.

The NICT TDC newsletter (IVS NICT-TDC News) is published on a non-regular basis by NICT.

This news was edited by Mamoru SEKIDO, Kashima Space Technology Center. Inquires on this issue should be addressed to Mamoru SEKIDO, Kashima Space Technology Center, National Institute of Information and Communications Technology, 893-1 Hirai, Kashima, Ibaraki 314-8501, Japan, e-mail : sekido@nict.go.jp.

Summaries of VLBI and related activities at the National Institute of Information and Communications Technology are on the Web. The URL to view the home page of the Radio Astronomy Applications Section of the Space-Time Measurement Group of Space-Time Standards Laboratory is : **"http://www2.nict.go.jp/sts/stmg/ivstdc/news-index.html"**.

IVS NICT TECHNOLOGY DEVELOPMENT CENTER NEWS No.39, January 2021

International VLBI Service for Geodesy and Astrometry
NICT Technology Development Center News
published by
National Institute of Information and Communications Technology, 4-2-1 Nukui-kita, Koganei, Tokyo 184-8795, Japan